Journal of Quantitative Spectroscopy & Radiative Transfer 112 (2011) 2079–2094

Contents lists available at ScienceDirect

Journal of Quantitative Spectroscopy & Radiative Transfer

journal homepage: www.elsevier.com/locate/jqsrt

Review

Directional radiometry and radiative transfer: A new paradigm

Michael I. Mishchenko *

NASA Goddard Institute for Space Studies, 2880 Broadway, New York, NY 10025, USA

ARTICLE INFO

Available online 5 May 2011

Keywords:
Electromagnetic scattering
Directional radiometry
Radiative transfer
Coherent backscattering
Optical particle characterization
Remote sensing
Macroscopic Maxwell equations

ABSTRACT

Measurements with directional radiometers and calculations based on the radiative transfer equation (RTE) have been at the very heart of weather and climate modeling and terrestrial remote sensing. The quantification of the energy budget of the Earth's climate system requires exquisite measurements and computations of the incoming and outgoing electromagnetic energy, while global characterization of climate system's components relies heavily on theoretical inversions of observational data obtained with various passive and active instruments. The same basic problems involving electromagnetic energy transport and its use for diagnostic and characterization purposes are encountered in numerous other areas of science, biomedicine, and engineering. Yet both the discipline of directional radiometry and the radiative transfer theory (RTT) have traditionally been based on phenomenological concepts many of which turn out to be profound misconceptions. Contrary to the widespread belief, a collimated radiometer does not, in general, measure the flow of electromagnetic energy along its optical axis, while the specific intensity does not quantify the amount of electromagnetic energy transported in a given direction.

The recently developed microphysical approach to radiative transfer and directional radiometry is explicitly based on the Maxwell equations and clarifies the physical nature of measurements with collimated radiometers and the actual content of the RTE. It reveals that the specific intensity has no fundamental physical meaning besides being a mathematical solution of the RTE, while the RTE itself is nothing more than an intermediate auxiliary equation. Only under special circumstances detailed in this review can the solution of the RTE be used to compute the time-averaged local Poynting vector as well as be measured by a collimated radiometer. These firmly established facts make the combination of the RTE and a collimated radiometer useful in a well-defined range of applications. However, outside the domain of validity of the RTT the practical usefulness of measurements with collimated radiometers remains uncertain, while the theoretical modeling of these measurements and the solution of the energy-budget problem require a more sophisticated approach than solving the RTE.

Published by Elsevier Ltd.

Contents

1. Introduction 2080
2. Specific intensity: is it a fundamental physical quantity? 2080
   2.1. Phenomenological specific intensity 2080
   2.2. Preisendorfer's radiance function 2081

Abbreviations: CB, coherent backscattering; DR, directional radiometry; MMEs, macroscopic Maxwell equations; PST, Poynting–Stokes tensor; QED, quantum electrodynamics; RT, radiative transfer; RTE, radiative transfer equation; RTT, radiative transfer theory; SI, specific intensity; VRTE, vector radiative transfer equation; WCR, well-collimated radiometer

* Tel.: +1 212 678 5590; fax: +1 212 678 5622.
E-mail addresses: mmishchenko@giss.nasa.gov, crmim2@gmail.com

0022-4073/$ - see front matter Published by Elsevier Ltd.
doi:10.1016/j.jqsrt.2011.04.006

3. Directional radiometers: what do they actually measure? . . . 2082
4. What are the actual problems one needs to solve? . . . 2084
5. Radiation-budget problem. . . . 2084
6. The Poynting–Stokes tensor . . . 2084
7. Solution of the energy-budget problem . . . 2085
7.1. Hierarchy of typical time scales . . . 2085
7.1.1. Monochromatic fields . . . 2085
7.1.2. Quasi-monochromatic light . . . 2086
7.1.3. Configuration averaging. . . . 2086
7.2. Ergodicity, randomness, and statistical uniformity. . . . 2086
7.3. Far-field approximation . . . 2087
7.4. The limit $N \to \infty$ and the Twersky approximation . . . 2087
7.5. The ladder approximation . . . 2088
7.6. The final result. . . . 2089
7.7. Discussion. . . . 2089
8. Theoretical modeling of measurements with directional radiometers . . . 2090
9. Discussion and conclusions . . . 2091
Acknowledgments . . . 2092
References . . . 2092

1. Introduction

One cannot imagine modern weather, climate, and remote-sensing science without the radiative transfer theory (RTT) and directional radiometry (DR). Indeed, accurate quantification of the Earth's energy budget necessitates precise measurements and computations of the incoming and outgoing electromagnetic energy [1,2], while regional and global characterization of the Earth's atmosphere and surface has been based traditionally on theoretical inversions of ground-based, airborne, and satellite measurements of transmitted, scattered, and emitted radiation [3,4]. The same basic problems involving electromagnetic energy transport and its use for non-invasive diagnostic and characterization purposes are common to a great variety of science, biomedicine, and engineering disciplines [5–20].

According to the majority of existing monographs and textbooks, both RTT and DR are essentially complete disciplines, the remaining unresolved issues being of purely technical character. For example, in the second edition of *Atmospheric Radiation,* Goody and Yung [21] remarked that the 25 years that had passed since the first edition was published, there had been many altered perceptions, usually direct results of changing technologies, but fewer advances in fundamental ideas. Similarly, Thomas and Stamnes [22] claimed that "the subject of radiative transfer has matured to the point of being a well-developed tool", Zdunkovski et al. [23] noted that "radiative transfer theory has reached a high point of development", while Kokhanovsky [24] emphasized the well-established nature of the radiative transfer equation (RTE) by remarking that "the derivation of this equation for random media with discrete particles is simple".

Given this unanimity of climate and remote-sensing experts, it should be quite striking to find the following statement in a recent monograph written by leading authorities on classical and quantum optics: "In spite of the extensive use of the theory of radiative energy transfer, no satisfactory derivation of its basic equation (i.e., the RTE) from electromagnetic theory… has been obtained up to now" [25]. In fact, detailed analyses have exposed the phenomenological theories of DR and radiative transfer to be eclectic combinations of *ad hoc* concepts and principles that may appear to be plausible at first sight but fall apart upon systematic scrutiny [26–30]. This situation is, of course, quite unfortunate, given the widespread use of the RTE for almost 125 years [31,32].

The objective of this review is to draw the attention of a broad range of climate, atmospheric radiation, remote-sensing, and biomedical scientists as well as optical, electrical, and mechanical engineers to the recent emergence of a microphysical paradigm in DR and RTT based on direct and self-consistent application of the Maxwell equations.[1] This paradigm solves the long-standing problem of establishing the fundamental physical link between the RTT and DR on the one hand and macroscopic electromagnetics on the other. This development allows one to clarify the physical content of a measurement with a directional (i.e., well-collimated) radiometer (hereafter WCR) and its relation to the solution of the RTE. It also suggests that in many cases the reading of a WCR must be modeled using a much more sophisticated approach than the RTE and that the very applicability of WCRs in quantifying the energy budget of the Earth's climate system or any particulate medium can be problematic and requires a detailed analysis based on first principles.

2. Specific intensity: is it a fundamental physical quantity?

2.1. Phenomenological specific intensity

Alongside Henri Poincaré's principle of relativity, Max Planck's energy quanta represent the most profound paradigm-changing concept of the 20th century physics [33]. It is, therefore, not surprising that virtually all

[1] The word "microphysical" serves to emphasize the direct traceability of the new DR and RTT concepts from fundamental physics (in this case from the macroscopic Maxwell equations, or MMEs) not afforded by the phenomenological approach (see the detailed discussion in Ref. [30]).

accounts of the phenomenological RTT and DR and the underlying concept of the specific intensity (SI) are rooted in Max Planck's famous treatise on heat radiation [34]. On page 1 of the English edition of this book [35], one can find the following manifesto: "The state of the radiation at a given instant and at a given point of the medium cannot be represented… by a single vector (that is, a single directed quantity). All heat rays which at a given instant pass through the same point of the medium are perfectly independent of one another, and in order to specify completely the state of the radiation the intensity of radiation must be known in all the directions, infinite in number, which pass through the point in question." Based on this premise, Planck gave the classical definition of the SI $I(\mathbf{r},\hat{\mathbf{q}})$ by stating that the amount of radiant energy $\mathrm{d}E$ transported through an arbitrarily chosen differential element of area $\mathrm{d}S$ in the interior of a medium in directions confined to a differential element of solid angle $\mathrm{d}\Omega_{\hat{\mathbf{q}}}$, centered at the propagation direction $\hat{\mathbf{q}}$, during a differential time interval $\mathrm{d}t$ is given by

$$\mathrm{d}E = I(\mathbf{r},\hat{\mathbf{q}})\cos\theta\,\mathrm{d}S\,\mathrm{d}t\,\mathrm{d}\Omega_{\hat{\mathbf{q}}}, \tag{1}$$

where $\mathbf{r}$ is the position vector of the differential surface element and θ is the angle between $\hat{\mathbf{q}}$ and the normal $\hat{\mathbf{n}}$ to $\mathrm{d}S$ (Fig. 1a). This definition was eventually adopted in the classical works by Milne [36], Hopf [37], and Chandrasekhar [38] as well as in virtually all subsequent monographs on RTT and DR (e.g., [3,4,11,12,16,19–24,39–45]). Although in his treatise Planck specifically considered black-body electromagnetic radiation, his concept of the SI was extrapolated to encompass diffuse multiple scattering of light by cloudy and other particulate media. The typical physical model of this situation is the scattering of a quasi-monochromatic parallel beam of light (e.g., sunlight) by a cloud, as shown in Fig. 2. It is this physical model that will be the subject of our review.

It is important to recognize that Planck [34,35] used what is now called the semi-classical approach (e.g., [25,46,47]), wherein the matter is quantized while the electromagnetic field remains purely classical. This implies that Planck's concept of the polydirectional SI contradicts one of the fundamental laws of classical electromagnetics according to which at any given moment t the propagation of the electromagnetic energy at any observation point $\mathbf{r}$ is fully described by the Poynting vector given by the vector product of the local electric and magnetic field vectors: $\mathbf{S}(\mathbf{r},\ t) = \mathbf{E}(\mathbf{r},\ t)\times\mathbf{H}(\mathbf{r},\ t)$ [48–51]. The direction and magnitude of this vector can change in time, but at any given moment t the propagation of the electromagnetic energy at any point $\mathbf{r}$ is monodirectional. Averaging over time also yields a monodirectional vector $\langle\mathbf{S}(\mathbf{r},t)\rangle_t = \langle\mathbf{E}(\mathbf{r},t)\times\mathbf{H}(\mathbf{r},t)\rangle_t$.

The traditional phenomenological way of addressing this profound inconsistency is to claim that, in fact, the electromagnetic field must also be quantized, which, allegedly, results in the emergence of photons as localized and "independent" particles of the electromagnetic field forming a "photon gas" [52–55]. For example, Bohren and Clothiaux [56] write explicitly on page 186 that "radiometry is based on approximating electromagnetic radiation as a gas of photons". The SI is then claimed to quantify the instantaneous directional distribution of all the photons passing through the differential surface element $\mathrm{d}S$ in Fig. 1a. This approach, however, faces an equally insurmountable problem [26,28,57]. Indeed, the real photons appearing in quantum electrodynamics (QED) are neither Newtonian corpuscles nor Einstein's energy quanta localized at points in space [58–63]. Each QED photon is a quantum of a single normal mode of the electromagnetic field and as such occupies the entire quantization volume (e.g., the entire cloud) and cannot be localized [25,64]. As a consequence, the photons cannot be used to define the SI at an observation point $\mathbf{r}$ [26]. It is, therefore, not surprising that the RTE has never been derived directly from QED.

2.2. Preisendorfer's radiance function

Preisendorfer [65] and Ishimaru [66] attempted another way of relating the heuristic SI to the Poynting vector by admitting that the former cannot be defined at a specific moment t but rather must be the result of averaging over a sufficiently long period of time. They observed that in a turbid medium, particles are in constant motion and can also change their sizes, shapes, and orientations, thereby rendering the direction and magnitude of the Poynting vector at an observation point (Fig. 2) random functions of time. At certain moments the direction of the instantaneous Poynting vector can fall within the differential solid angle $\mathrm{d}\Omega_{\hat{\mathbf{q}}}$ in Fig. 1a. Therefore, Preisendorfer and Ishimaru concluded that an appropriate definition of the SI could be the time-averaged length of the Poynting vectors at $\mathbf{r}$ with directions falling within $\mathrm{d}\Omega_{\hat{\mathbf{q}}}$. More specifically, Preisendorfer's radiance function is defined as follows (see Fig. 1a):

$$N(\mathbf{r},\hat{\mathbf{q}}) = \frac{1}{\cos\theta}\lim_{\Delta S\to 0}\frac{1}{\Delta S}\lim_{\Delta\Omega_{\hat{\mathbf{q}}}\to 0}\frac{1}{\Delta\Omega_{\hat{\mathbf{q}}}}\lim_{T\to\infty}\frac{1}{T} \times\int_{\Delta S}\mathrm{d}S'\int_t^{t+T}\mathrm{d}t'\left|\mathbf{S}(\mathbf{r}',t')\right|\chi[\Delta\Omega_{\hat{\mathbf{q}}},\hat{\mathbf{s}}(\mathbf{r}',t')], \tag{2}$$

where $\hat{\mathbf{s}}(\mathbf{r},t') = \mathbf{S}(\mathbf{r},t')/\left|\mathbf{S}(\mathbf{r},t')\right|$ is the unit vector in the direction of $\mathbf{S}(\mathbf{r}',t')$ and

$$\chi[\Delta\Omega_{\hat{\mathbf{q}}},\hat{\mathbf{s}}(\mathbf{r}',t')] = \begin{cases} 1 & \text{if } \hat{\mathbf{s}}(\mathbf{r}',t')\in\Delta\Omega_{\hat{\mathbf{q}}}, \\ 0 & \text{otherwise.}\end{cases} \tag{3}$$

In the chapter "Connections with the Mainland", Preisendorfer [65] summarized the most fundamental weakness of the phenomenological RTT from the standpoint of "mainland physicists", viz., the absence of a detailed derivation of the RTE from first principles. Indeed, the traditional back-of-an-envelope "derivation" amounts to little more than the postulation of the RTE based on the belief that the SI exists as a fundamental physical quantity, *a priori* possesses the desirable properties, and can be used to evaluate the energy balance of a vaguely defined "small volume element" [28]. Preisendorfer attempted to use the MMEs in order to demonstrate that his radiance function $N(\mathbf{r},\hat{\mathbf{q}})$ satisfies the RTE. However, his derivation failed for several reasons, including the incorrect assumption that the instantaneous electric and magnetic field vectors at any point inside a turbid medium are always mutually orthogonal.

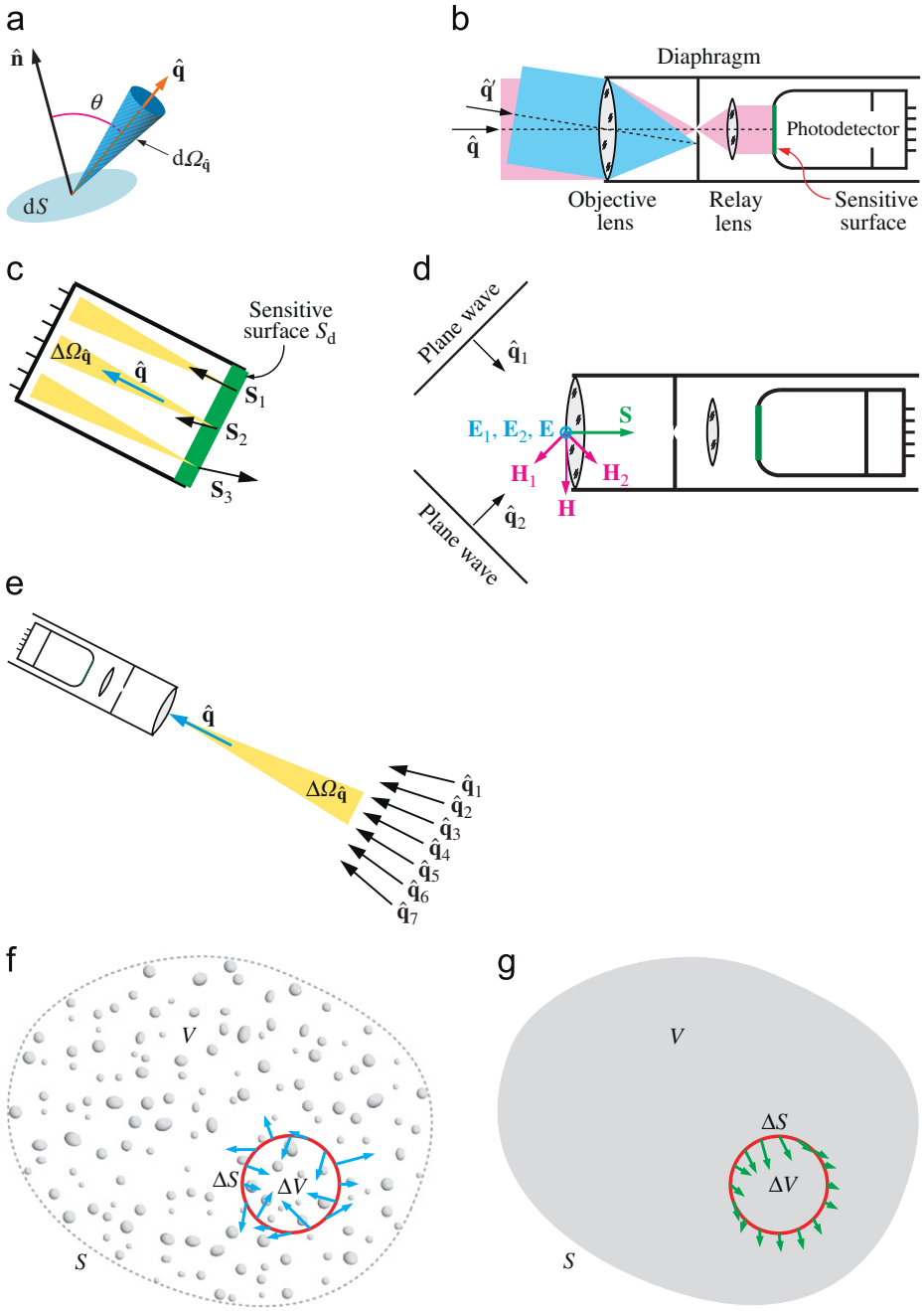

Fig. 1. (a) Definition of the phenomenological specific intensity, (b) typical optical scheme of a WCR, (c) hypothetical radiance function meter accumulating local Poynting vectors with directions falling within the acceptance solid angle $\Delta\Omega_{\hat{\mathbf{q}}}$. (d) The conventional WCR does not respond to the Poynting vector directed along the optical axis of the instrument. (e) Response of a WCR to a superposition of plane electromagnetic waves. (f) Instantaneous radiation budget of a volume element ΔV bounded by a closed surface ΔS. The arrows represent the instantaneous distribution of $\mathbf{S}(\mathbf{r},\ t)$ over ΔS corresponding to the specific multi-particle configuration occurring at the moment t. (g) Time-averaged radiation budget of the same volume element.

There is no doubt that if the SI was a fundamental, physically meaningful quantity then $N(\mathbf{r},\hat{\mathbf{q}})$ would be its most appropriate representation in terms of the Poynting vector. The unquestionable virtue of $N(\mathbf{r},\hat{\mathbf{q}})$ is that it possesses, by its very definition, one of the intended properties of the SI, viz., the integral of $N(\mathbf{r},\hat{\mathbf{q}})\hat{\mathbf{q}}$ over all directions $\hat{\mathbf{q}}$ yields the time-averaged Poynting vector at the observation point $\mathbf{r}$:

$$\langle \mathbf{S}(\mathbf{r},t)\rangle_t = \int_{4\pi} d\hat{\mathbf{q}}\hat{\mathbf{q}}N(\mathbf{r},\hat{\mathbf{q}}). \tag{4}$$

However, the decisive drawbacks of this quantity, as we shall see later, are that it cannot be measured with conventional WCRs and does not satisfy the RTE.

3. Directional radiometers: what do they actually measure?

A hypothetical instrument capable of measuring the radiance function $N(\mathbf{r},\hat{\mathbf{q}})$ is shown in Fig. 1c. The sensitive surface of this instrument S_d is exposed directly to the incoming radiation and is assumed to react to the local

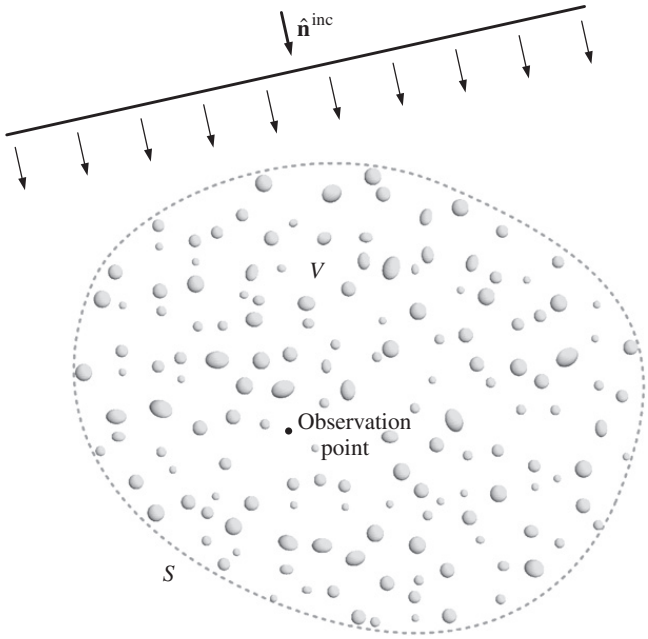

Fig. 2. A random cloud of N particles illuminated by a plane electromagnetic wave or a parallel quasi-monochromatic beam of light propagating in the direction of the unit vector $\hat{\mathbf{n}}^{\text{inc}}$.

instantaneous Poynting vector only if this vector is directed normally or almost normally to the surface. Specifically, if the direction of $\mathbf{S}(\mathbf{r}',t)$ at any point $\mathbf{r}'$ of the sensitive surface is within the small acceptance solid angle $\Delta\Omega_{\hat{\mathbf{q}}}$ of the detector (e.g., vector $\mathbf{S}_1$ in Fig. 1c) then this vector contributes to the cumulative reading of the instrument. Instantaneous local Poynting vectors with directions outside $\Delta\Omega_{\hat{\mathbf{q}}}$ (e.g., vectors $\mathbf{S}_2$ and $\mathbf{S}_3$) are ignored by the instrument and do not contribute to its reading. Obviously, accumulating the signal over a sufficiently long period of time T and dividing it by S_{d}, $\Delta\Omega_{\hat{\mathbf{q}}}$, and T directly yields $N(\mathbf{r},\hat{\mathbf{q}})$.

Thus, this hypothetical instrument is directly applicable, by its very definition, to the measurement of the radiance function $N(\mathbf{r},\hat{\mathbf{q}})$ and the local time-averaged Poynting vector via Eq. (4). If it were feasible, this instrument would serve as an ideal bridge between fundamental electromagnetics and the semi-empirical field of DR. Unfortunately, to the best of the author's knowledge, such an instrument has never been built, and it remains quite questionable whether it can be built in principle. Obviously, assessing the very feasibility of an instrument with directional sensitivity to the local instantaneous Poynting vector (Fig. 1c) requires an advanced quantum-mechanical analysis of light-matter interaction.

The actual WCRs in use today are based on a profoundly different physical principle, as shown in Fig. 1b. Let us consider two plane electromagnetic waves propagating in directions $\hat{\mathbf{q}}$ and $\hat{\mathbf{q}}'$, respectively. The objective lens transforms both plane wavefronts into converging spherical wavefronts with their respective focal points located in the plane of the diaphragm. The pink wavefront passes freely through the pinhole, is relayed onto the sensitive surface of the photodetector, and contributes to the resulting signal. On the other hand, the blue wavefront gets extinguished by the diaphragm and does not contribute to the reading of the detector.

Thus the combination {objective lens, diaphragm} serves to select only wavefronts propagating in directions very close to the optical axis of the instrument and falling within its small "acceptance" solid angle $\Delta\Omega = \pi d^2/(4f^2)$, where d is the diameter of the pinhole and f is the focal length of the objective lens. The fundamental difference between the two instruments shown in Fig. 1b and c is that the former selects appropriately directed wavefronts, whereas the latter selects appropriately directed Poynting vectors. It can thus be said that *the hypothetical radiance-function meter operates in the Poynting-vector domain, whereas the conventional WCR acts as a wave-domain filter* [67].

This analysis implies that the typical WCR does not necessarily react to the local Poynting vector at a point on the objective lens even if this vector is directed along the optical axis of the instrument. To demonstrate this, let us consider two plane electromagnetic waves propagating in directions $\hat{\mathbf{q}}_1$ and $\hat{\mathbf{q}}_2$ such that both form a 45° angle with the optical axis of the WCR (Fig. 1d). The waves are linearly polarized, with their electric vectors $\mathbf{E}_1$ and $\mathbf{E}_2$ oscillating perpendicularly to the paper, and fully coherent in that at any moment in time $\mathbf{E}_1 = \mathbf{E}_2$ in the central point of the objective lens. Let the local instantaneous magnetic vectors of the waves be $\mathbf{H}_1$ and $\mathbf{H}_2$, respectively, as shown by the magenta arrows, while the corresponding instantaneous electric vectors $\mathbf{E}_1 = \mathbf{E}_2$ are directed towards the reader. The cumulative local instantaneous field is represented by the vectors $\mathbf{E} = 2\mathbf{E}_1$ and $\mathbf{H} = \mathbf{H}_1 + \mathbf{H}_2$, the former again being directed towards the reader. One can see that the resulting local instantaneous Poynting vector $\mathbf{S} = \mathbf{E} \times \mathbf{H}$, shown by the green arrow, is directed along the optical axis of the instrument. Furthermore, it is easily verified that the Poynting vector at the central point is always directed along the optical axis of the WCR. Yet the reading of the detector will be identically equal to zero since neither plane wavefront is passed by the {objective lens, diaphragm} combination.

The failure of the WCR to react to the instantaneous Poynting vector in Fig. 1d can be traced to the following fundamental fact: although the Poynting vector is sought at points on the surface of the objective lens, the actual photodetector is invariably located very far (compared with the wavelength) from those points. What the optical scheme of the WCR can relay from the entrance plane onto the sensitive surface of the photodetector is a suitable plane (or quasi-plane) wavefront but not the Poynting vector of the *total* field. The only circumstance in which the WCR relays the Poynting vector itself is when the total field consists only of one or several plane electromagnetic waves propagating along the optical axis of the instrument.

This is true of any WCR irrespective of its particular optical scheme. In fact, it is the very principle of serving as a *wavefront angular filter* (rather than a Poynting-vector angular filter) that allows one to build a WCR by using easy-to-fabricate macroscopic optical elements (such as lenses, mirrors, polarizers, prisms, diffraction gratings, etc.).

Thus, contrary to the widespread belief, a WCR cannot be said to measure the directional distribution of the

electromagnetic energy flow at an observation point. It is, therefore, very important to formulate precisely what it does do. Let us assume that there are several plane wavefronts illuminating the objective lens of a WCR (Fig. 1e). According to the above discussion, the WCR does the following:

- selects only those wavefronts whose propagation directions fall within its small acceptance solid angle $\Delta\Omega_{\hat{\mathbf{q}}}$ (i.e., $\hat{\mathbf{q}}_3$, $\hat{\mathbf{q}}_4$, and $\hat{\mathbf{q}}_5$, but not $\hat{\mathbf{q}}_1$, $\hat{\mathbf{q}}_2$, $\hat{\mathbf{q}}_6$, and $\hat{\mathbf{q}}_7$);
- sums up the respective instantaneous electric and magnetic fields: $\mathbf{E}' = \mathbf{E}_3 + \mathbf{E}_4 + \mathbf{E}_5$ and $\mathbf{H}' = \mathbf{H}_3 + \mathbf{H}_4 + \mathbf{H}_5$; and finally
- accumulates the product $\mathbf{S}' = \mathbf{E}' \times \mathbf{H}' S_o$ (which is directed along the optical axis by definition) over time, where S_o is the area of the objective lens.

Thus, a WCR performs a well-defined operation that is by no means equivalent to accumulating appropriately directed local instantaneous Poynting vectors of the *total field in the entrance plane* (cf. Fig. 1c).

4. What are the actual problems one needs to solve?

Despite being poorly defined, the heuristic concept of the polydirectional SI has been viewed by some as worth keeping. This has led to several publications intended to identify a microphysical quantity that would satisfy the RTE and thereby might be considered a legitimate proxy for the phenomenological SI (e.g., [68,69]). However, those studies have not clarified the issue of the requisite non-negativity and physical measurability of such proxies, have not resolved the contradiction between the monodirectionality of the actual electromagnetic energy transport and the polydirectionality of the phenomenological SI concept, and could not establish the physical link between the RTT and the effect of coherent backscattering (CB) discussed below.

Fortunately, recent research has demonstrated that one does not need to use the SI as the fundamental point of departure and contemplate it as a primordial physical quantity *a priori* possessing certain desirable properties. Instead, one needs to focus on addressing the following *well-defined problems of actual practical importance*:

1. How to evaluate theoretically the time-averaged radiation-energy budget of a macroscopic volume of particulate medium?
2. Given the widespread practical use of WCRs, how to model theoretically the particular measurement afforded by a WCR and thereby clarify its ability to serve as (i) an energy-budget instrument and/or (ii) a diagnostic tool suitable for optical characterization of a particulate medium in laboratory, *in situ*, or remote-sensing studies?

Indeed, it is the solution of these two specific problems that one needs in the final analysis, the hypothetical "angular distribution of the local electromagnetic energy flow" being irrelevant and unnecessary in addition to being unphysical. As explained below, both problems can be and have been addressed by directly solving the MMEs [28,67].

5. Radiation-budget problem

The gist of the radiation-budget problem is shown in Fig. 1f and g paralleling Fig. 2. In order to characterize the instantaneous local directional flow of electromagnetic energy resulting from scattering by a complex particulate object such as a cloud, one must calculate the Poynting vector of the total electromagnetic field at a point $\mathbf{r}$ as the vector product of the instantaneous total electric and magnetic fields: $\mathbf{S}(\mathbf{r},\ t) = \mathbf{E}(\mathbf{r},\ t) \times \mathbf{H}(\mathbf{r},\ t)$. Then the instantaneous radiation budget of a macroscopic volume element ΔV of the cloud bounded by a closed surface ΔS (Fig. 1f) can be evaluated by integrating $\mathbf{S}(\mathbf{r},\ t)$ over ΔS :

$$W_{\Delta S}(t) = -\int_{\Delta S} \mathrm{d}S \mathbf{S}(\mathbf{r}, t) \cdot \hat{\mathbf{n}}(\mathbf{r}), \tag{5}$$

where $W_{\Delta S}(t) \geq 0$ is the net amount of electromagnetic energy entering the volume element ΔV per unit time, the central dot denotes an inner product, and $\hat{\mathbf{n}}(\mathbf{r})$ is the local outward normal to the surface. If $W_{\Delta S} = 0$ then the incoming radiation is balanced by the outgoing radiation. Otherwise there is absorption of electromagnetic energy inside the volume element. The radiation budget of the entire volume V occupied by the cloud is evaluated similarly, except now the integral in Eq. (5) is taken over the closed boundary S (Fig. 1f).

Both the direction and the magnitude of $\mathbf{S}(\mathbf{r},\ t)$ change in time owing to the following:

- time-harmonic dependence of the electric and magnetic fields,
- random phase and/or amplitude fluctuations of the incident quasi-monochromatic light, and
- temporal changes of the multi-particle configuration.

The result is a complex speckle pattern rapidly fluctuating in time (Fig. 1f). However, in the majority of practical applications one is interested in the time-averaged energy-flow pattern. To suppress the speckle and thereby isolate the static pattern relevant to radiation-budget applications (Fig. 1g), one must average $\mathbf{S}(\mathbf{r},\ t)$ over a sufficiently long time interval.

6. The Poynting–Stokes tensor

It is important to recognize that at any moment, the pair of the electric and magnetic fields $\{\mathbf{E}(\mathbf{r},\ t), \mathbf{H}(\mathbf{r},\ t)\}$ is the solution of the MMEs for the specific instantaneous multi-particle configuration such as that shown in Fig. 1f. If the numerically exact solution of the MMEs at all moments in time for the respective multi-particle configurations was known then the computation of the time-averaged Poynting vector $\langle \mathbf{S}(\mathbf{r},\ t) \rangle_t$ would be quite straightforward. This is, however, not the case in the majority of practical situations. Therefore, one has to resort to simplifying assumptions that enable a quasi-analytical solution of the MMEs leading to a

quasi-analytical computation of $\langle \mathbf{S}(\mathbf{r},\ t)\rangle_t$. The latter would ideally be formulated in terms of a closed-form equation for $\langle \mathbf{S}(\mathbf{r},\ t)\rangle_t$ allowing one to express $\langle \mathbf{S}(\mathbf{r},\ t)\rangle_t$ directly in the Poynting vector of the incident beam and, thus, to bypass an explicit numerical solution of the MMEs for a multi-particle group.

However, to accomplish this objective one needs to address first the following fundamental issue: forming the vector product of the electric and magnetic field vectors results in a quantity that does not carry specific information about the participating fields. This makes the Poynting vector a non-traceable quantity. Indeed, since quite different combinations of electric and magnetic field vectors can yield the same Poynting vector of the incident radiation, the latter cannot uniquely define the time average of the total Poynting vector at the observation point.

As was demonstrated in [67], this obstacle can be overcome by introducing a more fundamental and informative quantity than the Poynting vector, viz., the so-called Poynting–Stokes tensor (PST):

$$\overleftrightarrow{P}(\mathbf{r},t) = \mathbf{E}(\mathbf{r},t) \otimes \mathbf{H}(\mathbf{r},t), \tag{6}$$

where $\otimes$ denotes a dyadic product of two vectors. Indeed, this quantity turns out to be fully traceable by virtue of carrying sufficient information about the participating fields. Furthermore, it contains sufficient information to compute any actual optical observable. In particular, one has in Cartesian coordinates:

$$\mathbf{S}(\mathbf{r},t) = [P_{yz}(\mathbf{r},t) - P_{zy}(\mathbf{r},t)]\hat{\mathbf{x}} + [P_{zx}(\mathbf{r},t) - P_{xz}(\mathbf{r},t)]\hat{\mathbf{y}} + [P_{xy}(\mathbf{r},t) - P_{yx}(\mathbf{r},t)]\hat{\mathbf{z}}, \tag{7}$$

where $\hat{\mathbf{x}}$, $\hat{\mathbf{y}}$, and $\hat{\mathbf{z}}$ are the corresponding unit vectors. Taking the time average of both sides of this formula yields $\langle \mathbf{S}(\mathbf{r},t)\rangle_t$ in terms of $\langle \overleftrightarrow{P}(\mathbf{r},t)\rangle_t$.

7. Solution of the energy-budget problem

In general, the computation of the time-averaged PST is a very difficult problem. It can, however, be simplified by making several well-defined and traceable approximations, as summarized below. The complete derivation can be found in Refs. [28,67,70,71].

7.1. Hierarchy of typical time scales

The first approximation is to introduce a hierarchy $T_1 \ll T_2 \ll T_3$ of three typical time scales, resembling the famous Bogoliubov's hierarchy of relaxation times underlying modern physical kinetics [72]. The first time scale, T_1, is the period of time-harmonic oscillations of the purely monochromatic electromagnetic field described directly by the MMEs [48–51]. The second time scale, T_2, is the typical period of random fluctuations of the amplitudes and phases of the electric and magnetic fields of the incident quasi-monochromatic beam of light (Fig. 2). The third time scale, T_3, characterizes significant changes in the cloud such as variations in particle positions and/or orientations. The inequality $T_1 \ll T_2$ allows one to apply the monochromatic MMEs to quasi-monochromatic incident light, whereas the inequality $T_2 \ll T_3$ allows one to separate averaging over random fluctuations of the quasi-monochromatic incident light from averaging over particle characteristics such as positions, orientations, sizes, refractive indices, etc., as described below.

7.1.1. Monochromatic fields

The time-harmonic dependence of a monochromatic electromagnetic field is conveniently factorized by introducing complex electric and magnetic field vectors:

$$\mathbf{E}(\mathbf{r},t) = \mathrm{Re}[\mathbf{E}(\mathbf{r})\exp(-\mathrm{i}\omega t)],$$
$$\mathbf{H}(\mathbf{r},t) = \mathrm{Re}[\mathbf{H}(\mathbf{r})\exp(-\mathrm{i}\omega t)], \tag{8}$$

where Re denotes the real part, $\mathrm{i} = (-1)^{1/2}$, and ω is the angular frequency such that $T_1 = 2\pi/\omega$. The frequency-domain monochromatic Maxwell curl equations for the time-independent complex electric and magnetic field vectors $\mathbf{E}(\mathbf{r})$ and $\mathbf{H}(\mathbf{r})$ are as follows [48,50,51]:

$$\left.\begin{aligned} \nabla \times \mathbf{E}(\mathbf{r}) &= \mathrm{i}\omega\mu_0\mathbf{H}(\mathbf{r}) \\ \nabla \times \mathbf{H}(\mathbf{r}) &= -\mathrm{i}\omega\varepsilon_1\mathbf{E}(\mathbf{r}) \end{aligned}\right\} \mathbf{r} \in V_{\mathrm{EXT}}, \tag{9a}$$

$$\left.\begin{aligned} \nabla \times \mathbf{E}(\mathbf{r}) &= \mathrm{i}\omega\mu_0\mathbf{H}(\mathbf{r}) \\ \nabla \times \mathbf{H}(\mathbf{r}) &= -\mathrm{i}\omega\varepsilon_2(\mathbf{r},\omega)\mathbf{E}(\mathbf{r}) \end{aligned}\right\} \mathbf{r} \in V_{\mathrm{INT}}. \tag{9b}$$

In these equations, V_{INT} is the cumulative "interior" volume occupied by the particulate scattering object (Fig. 2):

$$V_{\mathrm{INT}} = \bigcup_{i=1}^{N} V_i, \tag{10}$$

where V_i is the volume occupied by the ith particle; V_{EXT} is the infinite exterior region such that $V_{\mathrm{INT}} \cup V_{\mathrm{EXT}} = \Re^3$, where $\Re^3$ denotes the entire three-dimensional space; the host medium and the scattering object are assumed to be nonmagnetic; μ_0 is the permeability of a vacuum; ε_1 is the real-valued electric permittivity of the host medium; and $\varepsilon_2(\mathbf{r},\omega)$ is the complex permittivity of the object. Note that the host medium is assumed to be non-absorbing.

Let us assume that the incident light is a plane electromagnetic wave propagating in the direction of the unit vector $\hat{\mathbf{n}}^{\mathrm{inc}}$ (Fig. 2):

$$\mathbf{E}^{\mathrm{inc}}(\mathbf{r}) = \mathbf{E}_0^{\mathrm{inc}}\exp(\mathrm{i}k_1\hat{\mathbf{n}}^{\mathrm{inc}}\cdot\mathbf{r}), \tag{11a}$$

$$\mathbf{H}^{\mathrm{inc}}(\mathbf{r}) = \mathbf{H}_0^{\mathrm{inc}}\exp(\mathrm{i}k_1\hat{\mathbf{n}}^{\mathrm{inc}}\cdot\mathbf{r}) = \frac{k_1}{\omega\mu_0}\hat{\mathbf{n}}^{\mathrm{inc}}\times\mathbf{E}^{\mathrm{inc}}(\mathbf{r}), \tag{11b}$$

where $k_1 = \omega(\varepsilon_1\mu_0)^{1/2}$ is the wave number. The linearity of the MMEs implies that the electric and magnetic field vectors of the total field can be expressed in those of the incident field everywhere in space via the corresponding dyadic operators $\overleftrightarrow{E}$ and $\overleftrightarrow{H}$:

$$\mathbf{E}(\mathbf{r}) = \overleftrightarrow{E}(\mathbf{r},\hat{\mathbf{n}}^{\mathrm{inc}})\cdot\mathbf{E}_0^{\mathrm{inc}}, \tag{12a}$$

$$\mathbf{H}(\mathbf{r}) = \overleftrightarrow{H}(\mathbf{r},\hat{\mathbf{n}}^{\mathrm{inc}})\cdot\mathbf{H}_0^{\mathrm{inc}}. \tag{12b}$$

Let us now introduce the corresponding complex PSTs [67]:

$$\overleftrightarrow{P}^{\mathrm{inc}} = \tfrac{1}{2}\mathbf{H}_0^{\mathrm{inc}} \otimes [\mathbf{E}_0^{\mathrm{inc}}]^*, \tag{13}$$

$$\overleftrightarrow{P}(\mathbf{r}) = \tfrac{1}{2}\mathbf{H}(\mathbf{r}) \otimes [\mathbf{E}(\mathbf{r})]^*, \tag{14}$$

where the asterisk denotes a complex-conjugate value. From Eqs. (12) to (14), one easily derives

$$\overleftrightarrow{P}(\mathbf{r}) = \overleftrightarrow{H}(\mathbf{r},\hat{\mathbf{n}}^{\rm inc})\cdot \overleftrightarrow{P}^{\rm inc}\cdot[\overleftrightarrow{E}(\mathbf{r},\hat{\mathbf{n}}^{\rm inc})]^{\rm T*}, \tag{15}$$

where T denotes a transposed dyadic. Thus, if the dyadics $\overleftrightarrow{E}$ and $\overleftrightarrow{H}$ are known[2] then Eq. (15) yields the complex PST of the total field at any point in space. Furthermore, Eq. (15) implies the existence of a linear operator $\hat{T}$ transforming the PST of the incident wave into that of the total field:

$$\overleftrightarrow{P}(\mathbf{r}) = \hat{T}(\mathbf{r},\hat{\mathbf{n}}^{\rm inc})\overleftrightarrow{P}^{\rm inc}, \tag{16}$$

where $\hat{T}(\mathbf{r},\ \hat{\mathbf{n}}^{\rm inc})$ is independent of $\mathbf{E}_0^{\rm inc}$ and $\mathbf{H}_0^{\rm inc}$ and is fully determined by the incidence direction and the specific instantaneous configuration of the N particles forming the cloud.

It is easily seen that there are no analogs of Eqs. (15) and (16) for the Poynting vector. This factor makes the Poynting vector a non-traceable quantity, as was discussed in Section 6.

As usual [48–51], the frequency-domain formula (14) implies that the real-valued PST averaged over a time interval Δt_1 much longer than the period of time-harmonic oscillations T_1 is given by

$$\langle \overleftrightarrow{P}(\mathbf{r},t)\rangle_{\Delta t_1} = {\rm Re}[\overleftrightarrow{P}(\mathbf{r})]^{\rm T}. \tag{17}$$

7.1.2. Quasi-monochromatic light

Although the complex fields $\mathbf{E}(\mathbf{r})$ and $\mathbf{H}(\mathbf{r})$ are independent of time for perfectly monochromatic radiation (e.g., a continuous laser beam), they may vary with time implicitly by fluctuating around their respective mean values in the more general case of quasi-monochromatic light (e.g., sunlight). However, these random oscillations occur over time intervals of the order of $T_2 \gg T_1$, i.e., much more slowly than the time-harmonic oscillations of the factor $\exp(-{\rm i}\omega t)$. The inequality $T_2 \gg \Delta t_1 \gg T_1$ allows one to formulate the scattering problem at any moment in terms of the monochromatic frequency-domain MMEs (9a) and (9b). The corresponding near-instantaneous (i.e., averaged over a sufficiently large number of time-harmonic oscillations captured by the time interval Δt_1) solution of the radiation-budget problem is then given by Eqs. (16) and (17).

Furthermore, if the N-particle configuration remains fixed over a time interval Δt_2 such that $T_2 \ll \Delta t_2 \ll T_3$ then the linear transformation operator $\hat{T}$ remains constant, and averaging Eq. (16) over Δt_2 yields

$$\langle \overleftrightarrow{P}(\mathbf{r})\rangle_{\Delta t_2} = \hat{T}(\mathbf{r},\hat{\mathbf{n}}^{\rm inc})\langle \overleftrightarrow{P}^{\rm inc}\rangle_{\Delta t_2}. \tag{18}$$

In other words, the complex PSTs of the incident and total fields in Eq. (16) are replaced by their respective time averages. Eq. (17) now takes the form

$$\langle \overleftrightarrow{P}(\mathbf{r},t)\rangle_{\Delta t_2} = {\rm Re}[\langle \overleftrightarrow{P}(\mathbf{r})\rangle_{\Delta t_2}]^{\rm T}. \tag{19}$$

[2] Note that according to Eqs. (9a) and (9b), these dyadics are not independent; one can be expressed in terms of the other.

7.1.3. Configuration averaging

Finally, averaging Eq. (18) over a time interval $\Delta t_3 \gg T_3$ does not affect $\langle \overleftrightarrow{P}^{\rm inc}\rangle_{\Delta t_2}$ but changes $\hat{T}(\mathbf{r},\ \hat{\mathbf{n}}^{\rm inc})$. The result is as follows:

$$\langle \overleftrightarrow{P}(\mathbf{r})\rangle_{\Delta t_3} = \langle \hat{T}(\mathbf{r},\hat{\mathbf{n}}^{\rm inc})\rangle_{\Delta t_3}\langle \overleftrightarrow{P}^{\rm inc}\rangle_{\Delta t_2}, \tag{20}$$

$$\langle \overleftrightarrow{P}(\mathbf{r},t)\rangle_{\Delta t_3} = {\rm Re}[\langle \overleftrightarrow{P}(\mathbf{r})\rangle_{\Delta t_3}]^{\rm T}. \tag{21}$$

Eq. (20) makes it quite explicit that the operator $\hat{T}(\mathbf{r},\ \hat{\mathbf{n}}^{\rm inc})$ is computed by solving the frequency-domain MMEs and that averaging this operator over time is totally separated from averaging over time the complex PST of the incident quasi-monochromatic light. In the particular case of purely monochromatic incident light, $\overleftrightarrow{P}^{\rm inc}$ is constant:

$$\langle \overleftrightarrow{P}(\mathbf{r})\rangle_{\Delta t_3} = \langle \hat{T}(\mathbf{r},\hat{\mathbf{n}}^{\rm inc})\rangle_{\Delta t_3}\overleftrightarrow{P}^{\rm inc}. \tag{22}$$

Comparison of Eq. (22) with Eq. (20) demonstrates that the solution of the time-averaged radiation-budget problem in the case of quasi-monochromatic incident light is reduced to the solution of the same problem for the case of a plane incident wave followed by the replacement of $\overleftrightarrow{P}^{\rm inc}$ with $\langle \overleftrightarrow{P}^{\rm inc}\rangle_{\Delta t_2}$. Obviously, this simplification is quite important and useful.

7.2. Ergodicity, randomness, and statistical uniformity

Although a random multi-particle group can be described at any given moment in terms of a specific fixed configuration, during the time interval Δt_3 the group goes through an infinite sequence of evolving discrete configurations. This temporal evolution is often defined by an intricate system of equations representing the various physical and chemical processes in action. To incorporate the solution of this system of equations for each moment into the theoretical averaging procedure can be a formidable task and is almost never done. A far more practical approach in most cases is based on the assumption of ergodicity. Specifically, it is assumed in what follows that:

- the multi-particle scattering system can be adequately characterized at any moment by a finite set of physical parameters; and
- the scattering system is sufficiently variable in time and the time interval Δt_3 is sufficiently long that averaging the PST over this interval is essentially equivalent to averaging over an appropriate analytical probability distribution of the physical parameters characterizing the scattering system.

In other words, the second major approximation used in the solution of the radiation-budget problem is to assume that averaging over time for one specific realization of a random scattering process is equivalent to ensemble

averaging. This assumption can be summarized as follows:

$$\langle \overleftrightarrow{P}(\mathbf{r})\rangle_{\Delta t_3} = \langle \overleftrightarrow{P}(\mathbf{r})\rangle_{\mathbf{R},\xi} = \langle \hat{T}(\mathbf{r},\hat{\mathbf{n}}^{\rm inc})\rangle_{\mathbf{R},\xi}\langle \overleftrightarrow{P}^{\rm inc}\rangle_{\Delta t_2}, \tag{23}$$

where the subscript $\mathbf{R}$ denotes averaging over all particle coordinates and the subscript ξ denotes averaging over all particle states (i.e., morphologies, orientations, sizes, and refractive indices).

The assumption of ergodicity is supplemented by the assumptions of randomness and uniformity. Specifically, it is assumed that:

- the position and state of each particle are statistically independent of each other and of those of all the other particles, and
- the spatial distribution of the particles throughout the volume V is random and statistically uniform.

It is obvious that these latter assumptions imply a rather low packing density of the multi-particle group, since otherwise the positions and states of different particles as well as the position and state of an individual particle could become correlated. However, they simplify the problem in hand quite substantially by (i) allowing one to split the ensemble averaging of the PST into the averaging over particle states and that over particle positions; (ii) allowing one to average the PST over the state and position of each particle independently of all the other particles; and (iii) making all the positions of the N particles throughout the entire cloud volume V equally probable.

7.3. Far-field approximation

The differential form of the frequency-domain MMEs (9a) and (9b) does not offer an obvious analytical way of computing $\langle \overleftrightarrow{P}(\mathbf{r})\rangle_{\Delta t_3}$ by exploiting the fact that the scattering target shown in Fig. 2 consists of non-overlapping and potentially widely separated bodies (particles). The integral form of the MMEs (the so-called Foldy–Lax equations) turns out to be much more convenient since it allows one to decompose the total electric and magnetic fields at the observation point into the respective incident fields and "individual-particle contributions" [28,73–77]:

$$\mathbf{E}(\mathbf{r}) = \mathbf{E}^{\rm inc}(\mathbf{r}) + \sum_{i=1}^{N}\mathbf{E}_i(\mathbf{r}) \tag{24}$$

and similarly for $\mathbf{H}(\mathbf{r})$. Each ith partial field can, in turn, be represented mathematically as a superposition of contributions from all imaginable particle sequences ending at particle i:

$$\mathbf{E}_i = \mathbf{E}_{i0} + \sum_{j(\neq i)=1}^{N}\mathbf{E}_{ij} + \sum_{j(\neq i)=1}^{N}\sum_{k(\neq j)=1}^{N}\mathbf{E}_{ijk} + \cdots, \tag{25}$$

where $\mathbf{E}_{i0}$ is the "direct response" of particle i to the incident field. Examples of such "multiple-scattering" sequences are shown in Fig. 3a. Combining Eqs. (24) and (25) yields

$$\mathbf{E}(\mathbf{r}) = \mathbf{E}^{\rm inc}(\mathbf{r}) + \sum_{i=1}^{N}\mathbf{E}_{i0} + \sum_{i=1}^{N}\sum_{j(\neq i)=1}^{N}\mathbf{E}_{ij} + \sum_{i=1}^{N}\sum_{j(\neq i)=1}^{N}\sum_{k(\neq j)=1}^{N}\mathbf{E}_{ijk} + \cdots. \tag{26}$$

Note that decomposition (26) is purely mathematical and does not imply that multiple scattering is an actual physical phenomenon [57]. In other words, at any instant the MMEs "perceive" the entire cloud as a single scatterer rather than a collection of scatterers, even though the human eye classifies the cloud as consisting of "separate particles".

The explicit analytical expressions for the individual terms in decomposition (26) are still quite complex. They can, however, be drastically simplified upon making the following two assumptions:

- The N particles forming the group are separated widely enough that each of them is located in the far-field zones of all the other particles.
- The observation point is located in the far-field zone of any particle forming the group.

Specifically, we now have [28]

$$\begin{aligned}\mathbf{E}(\mathbf{r}) = {} & \mathbf{E}^{\rm inc}(\mathbf{r}) + \sum_{i=1}^{N}\frac{\exp(\mathrm{i}k_1 r_i)}{r_i}\overleftrightarrow{A}_i(\hat{\mathbf{r}}_i,\hat{\mathbf{n}}^{\rm inc})\cdot\mathbf{E}^{\rm inc}(\mathbf{R}_i) \\ & + \sum_{i=1}^{N}\sum_{j(\neq i)=1}^{N}\frac{\exp(\mathrm{i}k_1 r_i)}{r_i}\overleftrightarrow{A}_i(\hat{\mathbf{r}}_i,\hat{\mathbf{R}}_{ij})\cdot\frac{\exp(\mathrm{i}k_1 R_{ij})}{R_{ij}} \\ & \times\overleftrightarrow{A}_j(\hat{\mathbf{R}}_{ij},\hat{\mathbf{n}}^{\rm inc})\cdot\mathbf{E}^{\rm inc}(\mathbf{R}_j) + \cdots,\end{aligned} \tag{27}$$

where r_i is the distance between the origin of particle i and the observation point, $\hat{\mathbf{r}}_i$ is the unit vector directed from the origin of particle i towards the observation point, $\mathbf{R}_i$ is the position vector of the ith particle origin, R_{ij} is the distance between the origins of particles j and i, and $\hat{\mathbf{R}}_{ij}$ is the unit vector directed from the origin of particle j towards the origin of particle i (see Fig. 4). The quantity $\overleftrightarrow{A}_i(\hat{\mathbf{q}},\hat{\mathbf{q}}')$ is the standard scattering dyadic describing far-field scattering of a plane electromagnetic wave by particle i in the absence of all the other particles [28,76].

The obvious advantage of the far-field "order-of-scattering" expansion (27) (and the analogous decomposition of the magnetic field) is that the individual-particle scattering dyadics can be calculated by solving the MMEs for each particle separately, i.e., in the absence of all the other particles. The price for this simplicity is the requirement of low packing density: the particles must be separated widely enough to ensure that two neighboring particles are located in the far-field zones of each other.

7.4. The limit $N \to \infty$ and the Twersky approximation

The "order-of-scattering" expansions (26) and (27) allow one to represent the total electric (magnetic) field at a point in space as a sum of contributions arising from all possible particle sequences. The next major assumption, called the Twersky approximation [28,78], is that all sequences involving a particle more than once can be neglected. For example, the "self-avoiding" sequences (i)–(iii) in Fig. 3a are kept, whereas sequence (iv) is excluded. It is straightforward to demonstrate that the Twersky approximation is justified provided that the

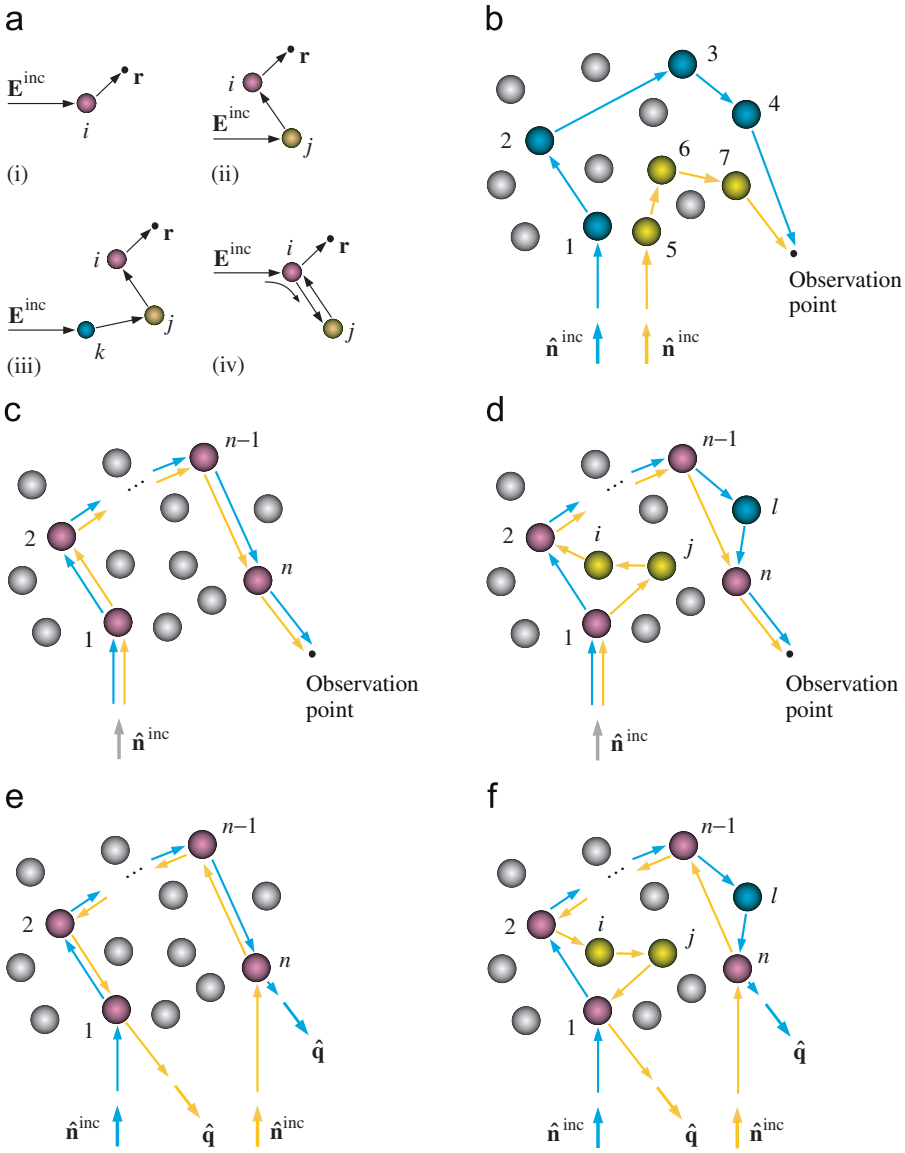

Fig. 3. (a) Examples of multi-particle sequences contributing to Eqs. (26) and (27). (b) Diagrams contributing to the PST of the total field. (c, d) Ladder diagrams. (e, f) Cyclical diagrams.

number of particles in the scattering volume is very large. Thus, instead of Eq. (26), we have

$$\mathbf{E}(\mathbf{r}) = \mathbf{E}^{\mathrm{inc}}(\mathbf{r}) + \sum_{i=1}^{N} \mathbf{E}_{i0} + \sum_{i=1}^{N} \sum_{\substack{j=1 \\ j\neq i}}^{N} \mathbf{E}_{ij} + \sum_{i=1}^{N} \sum_{\substack{j=1 \\ j\neq i}}^{N} \sum_{\substack{k=1 \\ k\neq i \\ k\neq j}}^{N} \mathbf{E}_{ijk} + \cdots. \tag{28}$$

Eq. (27) is simplified analogously. Note that the very applicability of the Twersky approximation makes the limit $N \to \infty$ an explicit assumption in the solution of the energy-budget problem for a multi-particle cloud.

7.5. The ladder approximation

It is clear from the above that the computation of the time-averaged PST involves ensemble averaging of dyadic products of the type $\mathbf{H}_{i\ldots k} \otimes \mathbf{E}^*_{l\ldots m}$. Each such product can be depicted diagrammatically as shown in Fig. 3b. The magnetic-field term $\mathbf{H}_{4321}$ is represented by blue arrows, while the electric-field term $\mathbf{E}^*_{765}$ is shown by yellow arrows. The essence of the so-called ladder approximation is to keep only a certain class of diagrams. The simplest ladder diagram is shown in Fig. 3c and corresponds to the product $\mathbf{H}_{n,n-1,\ldots 2,1} \otimes \mathbf{E}^*_{n,n-1,\ldots 2,1}$. In other words, all n particles are common to the corresponding magnetic- and electric-field terms and appear in exactly the same order. Fig. 3d shows a more complicated ladder diagram in which the same n particles are common to both terms and appear in the same order. However, the magnetic-field sequence contains an additional uncommon particle, while the electric-field sequence contains two uncommon particles. Obviously, this diagram corresponds to the product $\mathbf{H}_{n,l,n-1,\ldots,2,1} \otimes \mathbf{E}^*_{n,n-1,\ldots,2,i,j,1}$. Thus, the main characteristic of the ladder diagrams is that all common particles appear in corresponding magnetic- and electric-field sequences in exactly the same order.

The main justification for using the ladder approximation is that averaging over random positions of participating particles can be expected to extinguish the

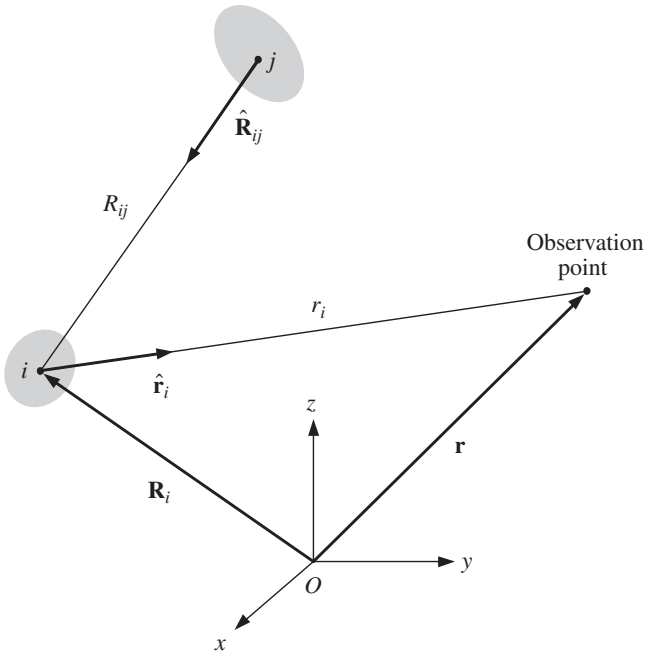

Fig. 4. Notation used in Eq. (27).

contribution of any multi-particle diagram with no common particles appearing in the same order, like, e.g., the diagram shown in Fig. 3b.

7.6. The final result

The above assumptions and approximations make it possible to solve the time-averaged radiation-budget problem analytically using the MMEs as the fundamental point of departure. Again, the complete derivation can be found in Refs. [28,67], while here we present only the final result.

Specifically, the time-averaged Poynting vector at the observation point $\mathbf{r}$ (Fig. 2) is given by the following integral over all directions of the unit vector $\hat{\mathbf{q}}$:

$$\langle \mathbf{S}(\mathbf{r},t)\rangle_{\Delta t_3} = \langle \mathbf{S}(\mathbf{r},t)\rangle_{\mathbf{R},\xi} = \int_{4\pi} \mathrm{d}\hat{\mathbf{q}}\hat{\mathbf{q}}\tilde{I}(\mathbf{r},\hat{\mathbf{q}}). \tag{29}$$

The non-negative function $\tilde{I}(\mathbf{r},\hat{\mathbf{q}})$ appearing in the integrand is the first element of a four-element real-valued column $\tilde{\mathbf{I}}(\mathbf{r},\hat{\mathbf{q}})$ which satisfies the following integro-differential equation:

$$\hat{\mathbf{q}}\cdot\nabla\tilde{\mathbf{I}}(\mathbf{r},\hat{\mathbf{q}}) = -n_0\langle \mathbf{K}(\hat{\mathbf{q}})\rangle_\xi \tilde{\mathbf{I}}(\mathbf{r},\hat{\mathbf{q}}) + n_0\int_{4\pi} \mathrm{d}\hat{\mathbf{q}}'\langle \mathbf{Z}(\hat{\mathbf{q}},\hat{\mathbf{q}}')\rangle_\xi \tilde{\mathbf{I}}(\mathbf{r},\hat{\mathbf{q}}'). \tag{30}$$

In this equation, $n_0 = N/V$ is the average number of particles per unit volume, $\langle \mathbf{K}(\hat{\mathbf{q}})\rangle_\xi$ is the 4×4 single-particle extinction matrix averaged over all states of all the N particles, and $\langle \mathbf{Z}(\hat{\mathbf{q}},\hat{\mathbf{q}}')\rangle$ is the 4×4 single-particle phase matrix, also averaged over all particle states. All elements of the extinction and phase matrices are real-valued. Eq. (30) must be supplemented by appropriate boundary conditions on the closed surface S (Fig. 2) specifying the illumination conditions.

7.7. Discussion

The final result summarized in Section 7.6 is in fact quite remarkable. Indeed, Eq. (30) is mathematically the same as the standard vector RTE (VRTE) introduced phenomenologically by Rosenberg [79] (the simplified form of the VRTE corresponding to the case of Rayleigh particles was introduced by Chandrasekhar [38]). It is also seen that Eq. (29) is mathematically the same as Eq. (4). Furthermore, all elements of the four-component column $\tilde{\mathbf{I}}(\mathbf{r},\hat{\mathbf{q}})$, including $\tilde{I}(\mathbf{r},\hat{\mathbf{q}})$, have the standard dimension of the phenomenological SI: $\mathrm{W\,m^{-2}\,sr^{-1}}$. Therefore, one may be tempted to equate the phenomenological SI $I(\mathbf{r},\hat{\mathbf{q}})$ and the auxiliary mathematical function $\tilde{I}(\mathbf{r},\hat{\mathbf{q}})$. One should remember, however, that despite being numerically the same, these two quantities have profoundly different physical definitions: the former is postulated to be a primordial physical quantity, whereas the latter emerges as the solution of an intermediate mathematical equation.

Indeed, as we have already discussed, the traditional phenomenological definition of the SI states that $I(\mathbf{r},\hat{\mathbf{q}})$ gives the amount of electromagnetic energy transported in the direction $\hat{\mathbf{q}}$ per unit area normal to $\hat{\mathbf{q}}$ per unit time per unit solid angle. This notion of the SI implies that at the observation point $\mathbf{r}$, the instantaneous flow of electromagnetic energy occurs simultaneously in all directions according to the angular distribution function $I(\mathbf{r},\hat{\mathbf{q}})$. Our microphysical solution of the radiation-budget problem reveals that this phenomenological notion is profoundly incorrect. Indeed, the quantity $\tilde{I}(\mathbf{r},\hat{\mathbf{q}})$ appears only in the context of averaging the PST over a sufficiently long time interval $\Delta t_3 \gg T_3$ rather than characterizes the instantaneous radiation field. Furthermore, the instantaneous local flow of electromagnetic energy as well as any time average of this flow is inherently monodirectional.

This fundamental discrepancy between the phenomenological and microphysical approaches is not surprising. Indeed, the computation of the local electromagnetic energy flow in the framework of the microphysical approach is based on a step-by-step solution of the MMEs without invoking any *ad hoc* principles and concepts not contained in macroscopic electromagnetics. As a consequence, $\tilde{I}(\mathbf{r},\hat{\mathbf{q}})$ emerges as a purely mathematical quantity entering Eq. (29) and satisfying the auxiliary Eq. (30). As such, $\tilde{I}(\mathbf{r},\hat{\mathbf{q}})$ has no independent physical meaning. To state otherwise is equivalent to claming independent physical meaning for expansion coefficients appearing in an *ad hoc* mathematical expansion of a function in, e.g., Legendre or Chebyshev polynomials. The same is true of Eq. (30): it is just an intermediate mathematical equation that one has to solve in order to complete the computation of $\langle \mathbf{S}(\mathbf{r},\ t)\rangle_{\mathbf{R},\xi}$ in the framework of macroscopic electromagnetics.

The phenomenological approach turns everything upside down:

- the existence of the SI as a fundamental physical quantity is postulated at the very outset;
- the scalar RTE is "derived" as an outcome of verbal "energy balance considerations" and then modified to account for polarization by postulating the VRTE; and

- the MMEs are invoked only at the very last stage in order to compute, on an *ad hoc* basis, the average single-particle extinction and phase matrices.

In other words, the MMEs are treated as a supplement to the phenomenological theory rather than as primordial physical equations fully controlling all aspects of the interaction of macroscopic electromagnetic fields with a macroscopic particulate medium.

To illustrate the purely mathematical and auxiliary nature of the function $\tilde{I}(\mathbf{r},\ \hat{\mathbf{q}})$, let us consider the radiance function introduced by Preisendorfer [65]. As we have seen in Section 2.2, this function yields the time-averaged Poynting vector according to Eq. (4), the latter being mathematically the same as Eq. (29). Yet, $N(\mathbf{r},\hat{\mathbf{q}}) \neq \tilde{I}(\mathbf{r},\hat{\mathbf{q}})$. To show that, let us recall that the microphysical derivation of the time-averaged Poynting vector is based on the complex-vector frequency-domain formalism. This approach allows one to conveniently factor out the time-harmonic dependence of the electric and magnetic fields, but necessitates the primordial definition of the Poynting vector and the PST as averages over a sufficiently large number of time-harmonic oscillations captured by the time interval Δt_1 (Section 7.1.1). This means that the frequency-domain formalism cannot be used to evaluate the integrals in Eq. (2). Indeed, time-harmonic oscillations of the electric and magnetic vectors cause a rapidly oscillating Poynting vector at the observation point. At certain moments $\mathbf{S}(\mathbf{r},\ t)$ can be directed along $\hat{\mathbf{q}}$ and thereby contribute to $N(\mathbf{r},\hat{\mathbf{q}})$, while at other moments it can be directed along $-\hat{\mathbf{q}}$ and contribute to $N(\mathbf{r},-\hat{\mathbf{q}})$. While these "opposing" contributions are accounted for and accumulated in the computation of $N(\mathbf{r},\hat{\mathbf{q}})$ and $N(\mathbf{r},-\hat{\mathbf{q}})$, they substantially (but, of course, not completely) cancel each other in the frequency-domain computation of $\tilde{I}(\mathbf{r},\hat{\mathbf{q}})$ and $\tilde{I}(\mathbf{r},-\hat{\mathbf{q}})$ owing to the primordial averaging over a large number of time-harmonic oscillations. Of course, the inequality $N(\mathbf{r},\hat{\mathbf{q}}) \neq \tilde{I}(\mathbf{r},\hat{\mathbf{q}})$ coupled with the mathematical uniqueness of solution of Eq. (30) implies that $N(\mathbf{r},\ \hat{\mathbf{q}})$ does not satisfy the standard RTE. It remains unknown whether a closed-form analytical equation for $N(\mathbf{r},\ \hat{\mathbf{q}})$ exists, but if it were derived then it would offer an alternative way of solving the time-averaged radiation-budget problem via Eq. (4).

This example illustrates the following important corollary of the microphysical approach: actual physical significance can be attributed only to the integral of $\hat{\mathbf{q}}\,\tilde{I}(\mathbf{r},\ \hat{\mathbf{q}})$ over all directions $\hat{\mathbf{q}}$ rather than to the particular values of $\tilde{I}(\mathbf{r},\hat{\mathbf{q}})$ corresponding to individual directions. For example, one can add to $\tilde{I}(\mathbf{r},\ \hat{\mathbf{q}})$ any function $f(\mathbf{r},\hat{\mathbf{q}})$ such that $\int_{4\pi} \mathrm{d}\hat{\mathbf{q}}\hat{\mathbf{q}} f(\mathbf{r},\hat{\mathbf{q}}) = \mathbf{0}$ and obtain another "specific intensity" yielding the same $\langle \mathbf{S}(\mathbf{r},t) \rangle_{\mathbf{R},\xi}$. A simple example would be any symmetric function such that $f(\mathbf{r},-\hat{\mathbf{q}}) = f(\mathbf{r},\hat{\mathbf{q}})$.

8. Theoretical modeling of measurements with directional radiometers

Let us now apply the same microphysical approach to model theoretically the reading of a WCR placed inside the random N-particle cloud (Fig. 5). Again, the instantaneous real electric and magnetic vectors at the surface of the objective lens can be represented as superpositions of the respective vectors of the incident field and the partial fields coming from all the individual particles

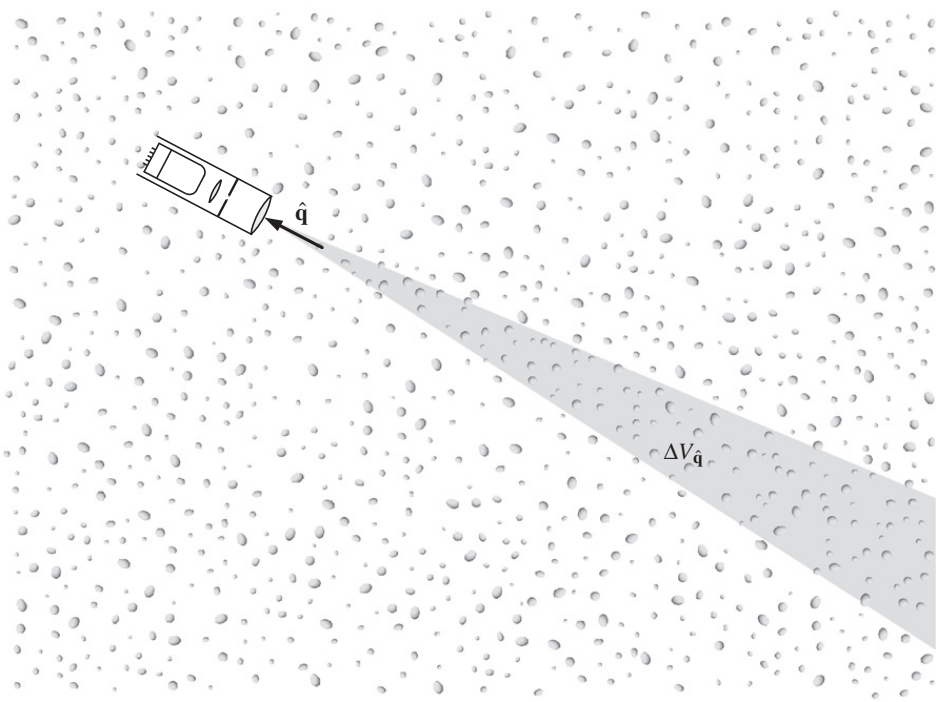

Fig. 5. A directional radiometer placed inside a random particulate medium.

(cf. Eq. (24)):

$$\mathbf{E}(\mathbf{r},t)=\mathbf{E}^{\rm inc}(\mathbf{r},t)+\sum_{i=1}^{N}\mathbf{E}_i(\mathbf{r},t),$$
$$\mathbf{H}(\mathbf{r},t)=\mathbf{H}^{\rm inc}(\mathbf{r},t)+\sum_{i=1}^{N}\mathbf{H}_i(\mathbf{r},t). \tag{31}$$

Since the observation point is assumed to be in the far-field zone of any particle, each pair $\{\mathbf{E}_i(\mathbf{r},t),\mathbf{H}_i(\mathbf{r},t)\}$ represents an outgoing spherical wavelet originating at the center of the respective particle. At a large distance from the particle this wavelet can be considered locally flat. Therefore, the radiometer will select only those wavelets that come from the particles located within the "acceptance volume" of the radiometer $\Delta V_{\hat{\mathbf{q}}}$ defined by its acceptance solid angle $\Delta\Omega_{\hat{\mathbf{q}}}$ (Fig. 5) and will integrate the resulting Poynting vector over the surface of the objective lens $S_{\rm o}$. Assuming for simplicity that $\Delta\Omega_{\hat{\mathbf{q}}}$ does not subtend the propagation direction of the incident light $\hat{\mathbf{n}}^{\rm inc}$, we conclude that the instantaneous reading of the WCR is given by $S_{\rm o}\sum_{l'}\sum_{m'}\mathbf{E}_{l'}(\mathbf{r},t)\times\mathbf{H}_{m'}(\mathbf{r},t)$, where the primed indices l' and m' number particles located inside the acceptance volume $\Delta V_{\hat{\mathbf{q}}}$. Note that since $\Delta\Omega_{\hat{\mathbf{q}}}$ is very small, each term in this sum is a vector directed essentially along the unit vector $\hat{\mathbf{q}}$ in Fig. 5. Accumulating this reading over the time interval Δt_3, dividing the result by Δt_3, and assuming ergodicity yields the following average signal per unit area of the objective lens:

$$\left\langle\sum_{l'}\sum_{m'}\mathbf{E}_{l'}(\mathbf{r},t)\times\mathbf{H}_{m'}(\mathbf{r},t)\right\rangle_{\Delta t_3}$$
$$=\frac{1}{2}{\rm Re}\left\langle\sum_{l'}\sum_{m'}\mathbf{E}_{l'}(\mathbf{r})\times[\mathbf{H}_{m'}(\mathbf{r})]^*\right\rangle_{\mathbf{R},\xi}, \tag{32}$$

where the subscripts $\mathbf{R}$ and ξ denote averaging over coordinates and states of all the N particles constituting the scattering medium and not just those located inside $\Delta V_{\hat{\mathbf{q}}}$.

The right-hand side of Eq. (32) can be expressed in terms of the following PST:

$$\overleftrightarrow{P}(\mathbf{r};\Delta V_{\hat{\mathbf{q}}})=\frac{1}{2}\left\langle\sum_{l'}\sum_{m'}\mathbf{H}_{l'}(\mathbf{r})\otimes[\mathbf{E}_{m'}(\mathbf{r})]^*\right\rangle_{\mathbf{R},\xi}. \tag{33}$$

We can compute this quantity by making all the standard assumptions invoked in Section 7 to calculate $\langle\overleftrightarrow{P}(\mathbf{r})\rangle_{\mathbf{R},\xi}$ and in addition requiring that the end particle of any scattering sequence in Eq. (27) be located inside the acceptance volume $\Delta V_{\hat{\mathbf{q}}}$. The result of this computation [67] is quite profound and implies that the reading of the WCR in Fig. 5 per unit time is given by the product $S_{\rm o}\Delta\Omega_{\hat{\mathbf{q}}}\tilde{I}(\mathbf{r},\ \hat{\mathbf{q}})$, where the unit vector $\hat{\mathbf{q}}$ is directed along the optical axis of the WCR and, as before, $\tilde{I}(\mathbf{r},\ \hat{\mathbf{q}})$ is the first element of the four-element column $\tilde{\mathbf{I}}(\mathbf{r},\ \hat{\mathbf{q}})$ satisfying Eq. (30).

The fundamental importance of this result, which applies to the case of quasi-monochromatic as well as monochromatic incident radiation, is difficult to overstate. Indeed, it means, first and foremost, that if all the above assumptions about the scattering particulate medium are valid then the WCR such as that shown in Fig. 5 measures the function $\tilde{I}(\mathbf{r},\ \hat{\mathbf{q}})$ provided that the reading of the radiometer is averaged over a sufficiently long period of time. Therefore, by sampling all incoming directions $\hat{\mathbf{q}}$, one can determine the local electromagnetic energy flow according to Eq. (29) and thereby solve the radiation-budget problem experimentally.

Secondly, the angular dependence of the measured function $\tilde{I}(\mathbf{r},\ \hat{\mathbf{q}})$ can be analyzed by solving Eq. (30) for a representative range of physical models of the scattering medium, which may yield certain information about the medium. Furthermore, since the WCR selects only locally plane wavefronts propagating in essentially the same direction $\hat{\mathbf{q}}$, one can add special optical elements and convert the WCR into a directional photopolarimeter capable of measuring the entire column vector $\tilde{\mathbf{I}}(\mathbf{r},\ \hat{\mathbf{q}})$. This measurement can contain additional implicit information about particle microphysics which can often be retrieved since the solution of Eq. (30) yields all four elements of $\tilde{\mathbf{I}}(\mathbf{r},\ \hat{\mathbf{q}})$ at once.

9. Discussion and conclusions

In the paper titled "Anti-photon" [63], Willis Lamb Jr. famously stated: "There is no such thing as a photon. Only a comedy of errors and historical accidents led to its popularity among physicists and optical scientists." What Lamb meant is that in most cases the word "photon" is taken out of its proper QED context and is used without clear understanding of what a QED photon actually is and, in particular, without realizing that it is not a localized particle of light. The QED photon represented a new paradigm brought about by the development of quantum electrodynamics by Paul Dirac, Werner Heisenberg, and Pascual Jordan in the late 1920s to the early 1930s [80–83], and the consequences of this major paradigm shift are still being evaluated [84].[3]

Paraphrasing Lamb, it can be said that "there is no such thing as specific intensity." Indeed, the very notion of polydirectional propagation of electromagnetic energy at a point in space contradicts basic laws of classical electromagnetics and does not follow from quantum electrodynamics. Furthermore, there is no practical need whatsoever to postulate the SI as a fundamental physical quantity in the first place; all relevant problems of actual practical significance can be solved without assuming the existence of the SI with its *a priori* defined properties.

As discussed in Section 4, there are two well-defined classes of practically important problems: radiation-budget problems and optical-characterization problems. Both types of problem can be addressed, in principle, by directly solving the MMEs. This solution yields the full electric and magnetic fields which can be used to compute the spatial and temporal distribution of the Poynting vector as well as to compute any optical observable.

In practice, this direct approach is often problematic, which calls for the introduction of appropriate simplifying

[3] I use the concepts of a scientific paradigm and a paradigm shift according to Gaston Bachelard. He introduced these profound notions in the 1930s using somewhat different terminology [85,86]. Kuhn [87] popularized Bachelard's ideas and re-instituted the use of the term "paradigm" introduced in Plato's dialog *Timaeus*.

assumptions. In the case of a sparse discrete random medium, the assumption listed in Section 7 allow one to address both classes of problem by expressing the spatial distribution of the time-averaged Poynting vector as well as the time-averaged reading of a WCR in terms of the solution of Eq. (30). Of course, one may be tempted to continue calling Eq. (30) "the radiative transfer equation" and the auxiliary mathematical function $\tilde{I}(\mathbf{r},\hat{\mathbf{q}})$ "the specific intensity" since Eq. (30) formally coincides with the phenomenologically postulated RTE and because $\tilde{I}(\mathbf{r},\hat{\mathbf{q}})$ happens to be *mathematically* identical to the phenomenologically postulated SI. One should always remember, however, that $\tilde{I}(\mathbf{r},\hat{\mathbf{q}})$ does not exist as a fundamental physical quantity allegedly describing an instantaneous polydirectional flow of electromagnetic energy at a point in space and that Eq. (30) is nothing more than an intermediate equation that one needs to solve in order to complete the computation of the time-averaged Poynting vector or to model the time-averaged reading of a WCR in the framework of classical electromagnetics.

Thus, our analysis reveals that the SI is not what it is postulated to be in the phenomenological RTT and that, contrary to a widespread belief, a WCR is not a universal radiance-function meter capable of yielding the time-averaged local Poynting vector via Eq. (4). It turns out, however, that in the case of electromagnetic scattering by an ergodic sparse discrete random medium:

- the time-averaged local Poynting vector can be found by evaluating the right-hand side of Eq. (29) in which $\tilde{I}(\mathbf{r},\ \hat{\mathbf{q}})$ (or, more generally, $\tilde{\mathbf{I}}(\mathbf{r},\ \hat{\mathbf{q}})$) is the solution of Eq. (30), the latter equation formally coinciding with the phenomenological VRTE; and
- the time-averaged reading of a WCR (or a directional photopolarimeter) is proportional to $\tilde{I}(\mathbf{r},\ \hat{\mathbf{q}})$ (or $\tilde{\mathbf{I}}(\mathbf{r},\ \hat{\mathbf{q}})$).

These firmly established facts make the combination of Eqs. (29) and (30) and a directional radiometer/photopolarimeter useful in a substantial range of radiation-budget and optical-characterization applications.

If one (or more) of the assumptions listed in Section 7 is violated then the solution of a radiation-budget or optical-characterization problem may require a more sophisticated theoretical approach and/or instruments other that a WCR. For example, the microphysical derivation of Eqs. (29) and (30) from the MMEs ignores the contribution of the so-called cyclical diagrams exemplified in Fig. 3e and f [88]. In this case particles 1, 2, …, n–1, n common to a pair of multi-particle sequences appear in the reverse order (cf. Fig. 3c and d). These cyclical diagrams can cause a significant CB effect [28,89–96] modifying the reading of a remote external WCR centered at the exact backscattering direction $\hat{\mathbf{q}} = -\hat{\mathbf{n}}^{\mathrm{inc}}$. The microphysical theory of CB and its relation to the microphysical RTT are outlined in detail in Refs. [18,28,97–104], while the remote-sensing implications of CB in planetary astrophysics are discussed in Refs. [18,105–121].

Another example is a densely packed particulate medium, in which case the far-field approximation (Section 7.3) may become inapplicable [117,122–126], thereby necessitating direct computer solutions of the MMEs [117,125–127].

Yet another example is near-field (micro- or nanoscale) electromagnetic energy transport [19,128–130]. In this case the very concept of a WCR as an energy-budget or optical-characterization instrument becomes fundamentally meaningless.

Acknowledgments

I thank Brian Cairns, Joop Hovenier, Michael Kahnert, Nikolai Khlebtsov, Pavel Litvinov, Dan Mackowski, Pinar Mengüç, Victor Tishkovets, and Larry Travis for numerous useful discussions and two anonymous reviewers for helpful comments. This basic research was funded by the NASA Radiation Sciences Program managed by Hal Maring and by the NASA Glory Mission project.

References

[1] Hansen JE, Nazarenko L, Ruedy R, et al. Earth's energy imbalance: confirmation and implications. Science 2005;308:1431–5.
[2] Trenberth KE, Fasullo JT, Kiehl J. Earth's global energy budget. Bull Am Meteorol Soc 2009;90:311–23.
[3] Stephens GL. Remote sensing of the lower atmosphere. New York: Oxford University Press; 1994.
[4] Liou KN. An introduction to atmospheric radiation. San Diego: Academic Press; 2002.
[5] Dolginov AZ, Gnedin Yu N, Silant'ev NA. Propagation and polarization of radiation in cosmic media. Basel: Gordon and Breach; 1995.
[6] Khlebtsov NG, Maksimova IL, Tuchin VV, Wang LV. Introduction to light scattering by biological objects. In: Tuchin VV, editor. Handbook of optical biomedical diagnostics. Bellingham, WA: SPIE Press; 2002. p. 31–167.
[7] Videen G, Kocifaj M, editors. Optics of cosmic dust. Dordrecht, The Netherlands: Kluwer; 2002.
[8] Modest MF. Radiative heat transfer. San Diego: Academic Press; 2003.
[9] Hanel RA, Conrath BJ, Jennings DE, Samuelson RE. Exploration of the solar system by infrared remote sensing. Cambridge, UK: Cambridge University Press; 2003.
[10] Videen G, Yatskiv Ya, Mishchenko M, editors. Photopolarimetry in remote sensing. Dordrecht, The Netherlands: Kluwer; 2004.
[11] Petty GW. A first course in atmospheric radiation. Madison, WI: Sundog Publishing; 2006.
[12] Mätzler C, editor. Thermal microwave radiation: applications for remote sensing. London: IET Press; 2006.
[13] Tuchin VV, Wang LV, Zimnyakov DA. Optical polarization in biomedical applications. Berlin: Springer; 2006.
[14] Hoekstra A, Maltsev V, Videen G, editors. Optics of biological particles. Dordrecht, The Netherlands: Springer; 2007.
[15] Tuchin V. Tissue optics. Bellingham, WA: SPIE Press; 2007.
[16] Dombrovsky LA, Baillis D. Thermal radiation in disperse systems: an engineering approach. Begell House; 2010.
[17] Wax A, Backman V, editors. Biomedical applications of light scattering. New York: McGraw-Hill; 2010.
[18] Mishchenko MI, Rosenbush VK, Kiselev NN, et al. Polarimetric remote sensing of solar system objects. Kyiv: Akademperiodyka; 2010. Available from: 〈http://www.giss.nasa.gov/~crmim/books.html〉.
[19] Howell JR, Siegel R, Mengüç MP. Thermal radiation heat transfer. Boca Raton, FL: CRC Press; 2011.
[20] Mishchenko MI, Yatskiv Ya S, Rosenbush VK, Videen G, editors. Polarimetric detection, characterization, and remote sensing. Berlin: Springer; 2011.
[21] Goody RM, Yung YL. Atmospheric radiation, theoretical basis. Oxford: Oxford University Press; 1989.
[22] Thomas GE, Stamnes K. Radiative transfer in the atmosphere and ocean. Cambridge, UK: Cambridge University Press; 1999.
[23] Zdunkovski W, Trautmann T, Bott A. Radiation in the atmosphere. Cambridge, UK: Cambridge University Press; 2007.
[24] Kokhanovsky A. Light scattering media optics. Berlin: Springer; 2004.

[25] Mandel L, Wolf E. Optical coherence and quantum optics. Cambridge, UK: Cambridge University Press; 1995.
[26] Wolf E. Coherence and radiometry. J Opt Soc Am 1978;68:6–17.
[27] Apresyan LA, Kravtsov Yu A. Radiation transfer. Statistical and wave aspects. Basel: Gordon and Breach; 1996.
[28] Mishchenko MI, Travis LD, Lacis AA. Multiple scattering of light by particles: radiative transfer and coherent backscattering. Cambridge, UK: Cambridge University Press; 2006.
[29] Mishchenko MI. Multiple scattering, radiative transfer, and weak localization in discrete random media: unified microphysical approach. Rev Geophys 2008;46:RG2003.
[30] Mishchenko MI, Tishkovets VP, Travis LD, et al. Electromagnetic scattering by a morphologically complex object: fundamental concepts and common misconceptions. J Quant Spectrosc Radiat Transfer 2011;112:671–92.
[31] Lommel E. Die Photometrie der diffusen Zurückwerfung. Sitzber Acad Wissensch München 1887;17:95–124.
[32] Chwolson O. Grundzüge einer mathematischen Theorie der inneren Diffusion des Lichtes. Bull l'Acad Impériale Sci St Pétersbourg 1889;33:221–56.
[33] Whittaker E. A history of the theories of aether and electricity. II. The modern theories. New York: Philosophical Library; 1954.
[34] Planck M. Theorie der Wärmestrahlung. Leipzig: Verlag Von Johann Ambrosius Barth; 1906.
[35] Planck M. The theory of heat radiation. Philadelphia: P. Blakiston's Son & Co; 1914.
[36] Milne E. Thermodynamics of the stars. Handbuch der Astrophysik 1930;3(Part 1):65–255.
[37] Hopf E. Mathematical problems of radiative equilibrium. Cambridge, UK: Cambridge University Press; 1934.
[38] Chandrasekhar S. Radiative transfer. Oxford: Oxford University Press; 1950.
[39] Sobolev VV. Light scattering in planetary atmospheres. Oxford: Pergamon Press; 1975.
[40] van de Hulst HC. Multiple light scattering. New York: Academic Press; 1980.
[41] Marchuk GI, Mikhailov GA, Nazaraliev MA, et al. The Monte Carlo methods in atmospheric optics. Berlin: Springer; 1980.
[42] Lenoble J. Atmospheric radiative transfer. Hampton, VA: A. Deepak Publishing; 1993.
[43] Yanovitskij EG. Light scattering in inhomogeneous atmospheres. Berlin: Springer; 1997.
[44] Hovenier JW, Van der Mee C, Domke H. Transfer of polarized light in planetary atmosphere—basic concepts and practical methods. Dordrecht, The Netherlands: Kluwer; 2004.
[45] Marshak A, Davis AB, editors. 3D radiative transfer in cloudy atmospheres. Berlin: Springer; 2005.
[46] Schiff LI. Quantum mechanics. New York: McGraw-Hill; 1968.
[47] Grynberg G, Aspect A, Fabre C. Introduction to quantum optics: from the semi-classical approach to quantized light. Cambridge, UK: Cambridge University Press; 2010.
[48] Stratton JA. Electromagnetic theory. New York: McGraw-Hill; 1941.
[49] Jackson JD. Classical electrodynamics. New York: Wiley; 1999.
[50] Van Bladel J. Electromagnetic fields. Piscataway, NJ: IEEE Press; 2007.
[51] Rothwell EJ, Cloud MJ. Electromagnetics. Boca Raton, FL: CRC Press; 2009.
[52] Pomraning GC. The equations of radiation hydrodynamics. Oxford: Pergamon Press; 1973.
[53] Mihalas D, Weibel-Mihalas B. Foundations of radiation hydrodynamics. Oxford: Oxford University Press; 1984.
[54] Oxenius J. Kinetic theory of particles and photons. Berlin: Springer; 1986.
[55] Pomraning GC. Linear kinetic theory and particle transport in stochastic mixtures. Singapore: World Scientific; 1991.
[56] Bohren CF, Clothiaux EE. Fundamentals of atmospheric radiation. Weinheim, Germany: Wiley; 2006.
[57] Mishchenko MI. Gustav Mie and the fundamental concept of electromagnetic scattering by particles: a perspective. J Quant Spectrosc Radiat Transfer 2009;110:1210–22.
[58] Bohm D. Quantum theory. Englewood Cliffs, NJ: Prentice-Hall; 1951.
[59] Kramers HA. Quantum mechanics. Amsterdam: North-Holland; 1957.
[60] Power EA. Introductory quantum electrodynamics. London: Longmans; 1964.
[61] Akhiezer AI, Berestetskii VB. Quantum electrodynamics. New York: Wiley; 1965.
[62] Kidd R, Ardini J, Anton A. Evolution of the modern photon. Am J Phys 1989;57:27–35.
[63] Lamb Jr WE. Anti-photon. Appl Phys B 1995;60:77–84.
[64] Meystre P, Sargent III M. Elements of quantum optics. Berlin: Springer; 1999.
[65] Preisendorfer RW. Radiative transfer on discrete spaces. Oxford: Pergamon Press; 1965.
[66] Ishimaru A. Wave propagation and scattering in random media. New York: Academic Press; 1978.
[67] Mishchenko MI. The Poynting–Stokes tensor and radiative transfer in discrete random media: the microphysical paradigm. Opt Express 2010;18:19,770–91.
[68] Fante RL. Relationship between radiative-transport theory and Maxwell's equations in dielectric media. J Opt Soc Am 1981;71: 460–8.
[69] Sudarshan ECG. Quantum theory of radiative transfer. Phys Rev A 1981;23:2802–9.
[70] Mishchenko MI. Vector radiative transfer equation for arbitrarily shaped and arbitrarily oriented particles: a microphysical derivation from statistical electromagnetics. Appl Opt 2002;41:7114–34.
[71] Mishchenko MI. Microphysical approach to polarized radiative transfer: extension to the case of an external observation point. Appl Opt 2003;42:4963–7.
[72] Bogoliubov NN. Problems of a dynamical theory in statistical physics. In: de Boer J, Uhlenbeck GE, editors. Studies in statistical mechanics, vol. I. Amsterdam: North-Holland; 1962. p. 1–118.
[73] Foldy LL. The multiple scattering of waves. Phys Rev 1945;67: 107–19.
[74] Lax M. Multiple scattering of waves. Rev Mod Phys 1951;23: 287–310.
[75] Tsang L, Kong JA, Shin RT. Theory of microwave remote sensing. New York: Wiley; 1985.
[76] Mishchenko MI, Travis LD, Lacis AA. Scattering, absorption, and emission of light by small particles. Cambridge, UK: Cambridge University Press; 2002. Available from: 〈http://www.giss.nasa.gov/~crmim/books.html〉.
[77] Babenko VA, Astafyeva LG, Kuzmin VN. Electromagnetic scattering in disperse media: inhomogeneous and anisotropic particles. Chichester, UK: Praxis; 2003.
[78] Twersky V. On propagation in random media of discrete scatterers. Proc Symp Appl Math 1964;16:84–116.
[79] Rozenberg G. Stokes vector-parameter. Uspekhi Fiz Nauk 1955; 56(1):77–110 [in Russian].
[80] Dirac PAM. The quantum theory of the emission and absorption of radiation. Proc R Soc London A 1927;114:243–65.
[81] Jordan P, Pauli W. Zur Quantenelektrodynamik ladungsfreier Felder. Z Phys 1928;47:151–73.
[82] Heisenberg W, Pauli W. Zur Quantendynamik der Wellenfelder. Z Phys 1929;56:1–61.
[83] Heisenberg W, Pauli W. Zur Quantentheorie der Wellenfelder. II. Z Phys 1930;59:168–90.
[84] Roychoudhury C, Kracklauer AF, Creath K, editors. The nature of light: what is a photon? Boca Raton, FL: CRC Press; 2008
[85] Bachelard G. The new scientific spirit. Boston: Beacon Press; 1984. (Original French edition: Le nouvel esprit scientifique. Paris: Presses Universitaires de France; 1934.
[86] Bachelard G. The formation of the scientific mind. Manchester: Clinamen Press; 2002. (Original French edition: La formation de l'esprit scientifique. Paris: Librairie Philosophique; 1938).
[87] Kuhn TS. The structure of scientific revolutions. New York: New American Library; 1986.
[88] Barabanenkov Yu N. Wave corrections to the transfer equation for back scattering. Radiophys Quantum Electron 1973;16:65–71.
[89] Kuga Y, Ishimaru A. Retroreflectance from a dense distribution of spherical particles. J Opt Soc Am A 1984;1:831–5.
[90] Wolf P, Maret G. Weak localization and coherent backscattering of photons in disordered media. Phys Rev Lett 1985;55:2696–9.
[91] van Albada MP, van der Mark MB, Lagendijk A. Observation of weak localization of light in a finite slab: anisotropy effects and light path classification. Phys Rev Lett 1987;58:361–4.
[92] van Albada MP, van der Mark MB, Lagendijk A. Polarization effects in weak localization of light. J Phys D 1988;21:S28–31.
[93] Barabanenkov Yu N. Kravtsov Yu A, Ozrin VD, Saichev AI. Enhanced backscattering in optics. Prog Opt 1991;29:65–197.
[94] van Tiggelen BA, Skipetrov SE, editors. Wave scattering in complex media: from theory to applications. Dordrecht, The Netherlands: Kluwer; 2003.
[95] Sheng P. Introduction to wave scattering, localization, and mesoscopic phenomena. Berlin: Springer; 2006.

[96] Akkermans E, Montambaux G. Mesoscopic physics of electrons and photons. Cambridge, UK: Cambridge University Press; 2007.
[97] Ozrin VD. Exact solution for coherent backscattering of polarized light from a random medium of Rayleigh scatterers. Waves Random Media 1992;2:141–64.
[98] Mishchenko MI. Enhanced backscattering of polarized light from discrete random media: calculations in exactly the backscattering direction. J Opt Soc Am A 1992;9:978–82.
[99] Amic E, Luck JM. Nieuwenhuizen ThM. Multiple Rayleigh scattering of electromagnetic waves. J Phys I (Fr) 1997;7:445–83.
[100] Tishkovets VP, Litvinov PV, Lyubchenko MV. Coherent opposition effect for semi-infinite discrete random medium in the double-scattering approximation. J Quant Spectrosc Radiat Transfer 2002; 72:803–11.
[101] Tishkovets VP, Mishchenko MI. Coherent backscattering of light by a layer of discrete random medium. J Quant Spectrosc Radiat Transfer 2004;86:161–80.
[102] Muinonen K. Coherent backscattering of light by complex random media of spherical scatterers: numerical solution. Waves Random Media 2004;14:365–88.
[103] Litvinov P, Tishkovets V, Ziegler K. Coherent backscattering effects for discrete random media. J Quant Spectrosc Radiat Transfer 2006;103:131–45.
[104] Tishkovets VP, Petrova EV, Mishchenko MI. Scattering of electromagnetic waves by ensembles of particles and discrete random media. J Quant Spectrosc Radiat Transfer 2011;112:2095–127.
[105] Shkuratov Yu G. A diffraction mechanism for the formation of the opposition effect of the brightness of surfaces having a complex structure. Kinem Fiz Nebes Tel 1988;4(4):33–9 [in Russian].
[106] Shkuratov Yu G. A new mechanism for the negative polarization of light scattered by the solid surfaces of cosmic bodies. Astron Vestnik 1989;23:176–80 [in Russian].
[107] Muinonen K. Light scattering by inhomogeneous media: backward enhancement and reversal of linear polarization. PhD dissertation, University of Helsinki, 1990.
[108] Mishchenko MI. Polarization characteristics of the coherent backscatter opposition effect. Earth Moon Planets 1992;58: 127–44.
[109] Mishchenko MI. On the nature of the polarization opposition effect exhibited by Saturn's rings. Astrophys J 1993;411:351–61.
[110] Mishchenko MI, Dlugach JM. Coherent backscatter and the opposition effect for E-type asteroids. Planet Space Sci 1993;41: 173–81.
[111] Shkuratov Yu G, Muinonen K, Bowell E, et al. A critical review of theoretical models of negatively polarized light scattered by atmosphereless solar system bodies. Earth Moon Planets 1994;65: 201–46.
[112] Rosenbush VK, Avramchuk VV, Rosenbush AE, Mishchenko MI. Polarization properties of the Galilean satellites of Jupiter: observations and preliminary analysis. Astrophys J 1997;487:402–14.
[113] Helfenstein P, Currier N, Clark BE, et al. Galileo observations of Europa's opposition effect. Icarus 1998;135:41–63.
[114] Rosenbush VK, Kiselev NN, Shevchenko VG, et al. Polarization and brightness opposition effects for the E-type asteroid 64 Angelina. Icarus 2005;178:222–34.
[115] Rosenbush VK, Kiselev NN. Polarization opposition effect for the Galilean satellites of Jupiter. Icarus 2005;179:490–6.
[116] Avramchuk VV, Rosenbush VK, Bul'ba TP. Photometric study of the major satellites of Uranus. Sol Syst Res 2007;41:186–202.
[117] Mishchenko MI, Dlugach JM, Liu L, et al. Direct solutions of the Maxwell equations explain opposition phenomena observed for high albedo solar system objects. Astrophys J 2009;705:L118–22.
[118] Rosenbush V, Shevchenko V, Kiselev N, et al. Polarization and brightness opposition effects for E-type asteroid 44 Nysa. Icarus 2009;201:655–65.
[119] Kiselev N, Rosenbush V, Velichko F, Zaitsev S. Polarimetry of the Galilean satellites and Jupiter near opposition. J Quant Spectrosc Radiat Transfer 2009;110:1713–8.
[120] Kolokolova L, Buratti B, Tishkovets V. Impact of coherent backscattering on the spectra of icy satellites of Saturn and the implications of its effects for remote sensing. Astrophys J 2010; 711:L71–4.
[121] Kolokolova L, Liu L, Buratti B, Mishchenko M. Modeling variations in the near-infrared spectra produced by the coherent backscattering effect. J Quant Spectrosc Radiat Transfer 2011;112: 2175–81.
[122] Tishkovets VP. Incoherent and coherent backscattering of light by a layer of densely packed random medium. J Quant Spectrosc Radiat Transfer 2007;108:454–63.
[123] Petrova E, Tishkovets V, Jockers K. Modeling of opposition effects with ensembles of clusters: interplay of various scattering mechanisms. Icarus 2007;188:233–45.
[124] Tishkovets VP. Light scattering by closely packed clusters: shielding of particles by each other in the near field. J Quant Spectrosc Radiat Transfer 2008;109:2665–72.
[125] Dlugach JM, Mishchenko MI, Liu L, Mackowski DW. Numerically-exact computer simulations of light scattering by densely packed, random particulate media. J Quant Spectrosc Radiat Transfer 2011;112:2068–78.
[126] Mackowski DW, Mishchenko MI. A multiple sphere *T*-matrix Fortran code for use on parallel computer clusters. J Quant Spectrosc Radiat Transfer 2011;112:2182–92.
[127] Mishchenko MI, Liu L, Mackowski DW, et al. Multiple scattering by random particulate media: exact 3D results. Opt Express 2007; 15:2822–36.
[128] Novotny L, Hecht B. Principles of nano-optics. Cambridge, UK: Cambridge University Press; 2006.
[129] Kaviani M. Heat transfer physics. Cambridge, UK: Cambridge University Press; 2008.
[130] Gaponenko SV. Introduction to nanophotonics. Cambridge, UK: Cambridge University Press; 2010.